

STUDY OF NATURAL CONVECTION HEAT TRANSFER FROM VERTICAL TRIANGULAR FIN ARRAYS

By

S. M. AKHLAQUE-E-RASUL



DEPARTMENT OF MECHANICAL ENGINEERING
BANGLADESH UNIVERSITY OF ENGINEERING AND TECHNOLOGY,
DHAKA, BANGLADESH.



STUDY OF NATURAL CONVECTION HEAT TRANSFER FROM VERTICAL TRIANGULAR FIN ARRAYS

By

S. M. AKHLAQUE-E-RASUL

A thesis
submitted to the department of Mechanical Engineering in partial fulfillment of the requirements
for the degree of
Master of Engineering in Mechanical Engineering.

**BANGLADESH UNIVERSITY OF ENGINEERING AND TECHNOLOGY,
Dhaka, Bangladesh.**

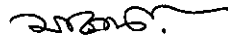
June, 1997

DEDICATED
TO
MY PARENTS AND WIFE

RECOMMENDATION OF THE BOARD OF EXAMINERS

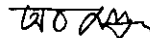
The board of examiners hereby recommends to the Department of Mechanical Engineering, BUET, Dhaka, acceptance of the thesis, "**STUDY OF NATURAL CONVECTION HEAT TRANSFER FROM VERTICAL TRIANGULAR FIN ARRAYS**", submitted by S. M. Akhlaque-E-Rasul, in partial fulfillment of the requirements for the degree of Master of Engineering in Mechanical Engineering.

Chairman (Supervisor) :




Dr. M. A. Rashid Sarkar
Professor
Dept. of Mech. Engg.
BUET, Dhaka

Member (Ex-officio) :



Dr. Amallesh Chandra Mandal
Professor and Head
Dept. of Mech. Engg.
BUET, Dhaka

Member :



Dr. A. M. Aziz-Ul-Huq
Professor
Dept. of Mech. Engg.
BUET, Dhaka

DECLARATION OF THE CANDIDATE

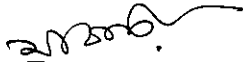
It is hereby declared that neither this thesis nor any part therefore has been submitted or is being concurrently submitted anywhere of the aware of any degree or diploma.



Candidate

CERTIFICATE OF RESEARCH

This is to certify that the work presented in this thesis is the outcome of the investigations carried out by the candidate under the supervision of Dr. M. A. Rashid Sarkar, Professor in the Department of Mechanical Engineering of Bangladesh University of Engineering & Technology, Dhaka, Bangladesh.



Supervisor



Candidate

ACKNOWLEDGEMENT

The author hereby expresses his very deep gratitude and acknowledges profound indebtedness to his supervisor Professor Dr. M. A. Rashid Sarkar, Department of Mechanical Engineering of Bangladesh University of Engineering and Technology (BUET) without whose continuous guidance, informal discussion, constant encouragement, it would not be possible for the author to finish the work

The author is highly grateful to Professor Dr. A. M. Aziz-Ul Huq, Department of Mechanical Engineering of Bangladesh University of Engineering & Technology (BUET) for his valuable assistance; fruitful suggestion in completing the work.

The author heartily acknowledge the assistance of personnel of welding shop and machine shop for improving the apparatus.

The author also remember the help of Engr. Rezaul Haque of Central Instrument Lab. and Mr. Dewan Md. Amir Hossain, Senior Lab. Instructor-Cum-Store Keeper of Heat Transfer Laboratory specially and express heartiest gratitude.

ABSTRACT

Experimental investigations of natural convection heat transfer from vertical triangular fin arrays, namely an array of four fins, an array of seven fins and an array of thirteen fins were carried out. All the fin arrays were prepared by sand casting. The fin dimensions in the arrays were: Length = 0.215m, Base thickness = 0.01m and Height = 0.04m.

The experimental regime parameters of this investigation were: $0.15 \text{ w/m}^2 < \text{Heat Flux} < 180 \text{ w/m}^2$; $0.1^\circ\text{C} < \text{Temperature Difference } (\Delta T) < 15^\circ\text{C}$ and $0.1 < \text{Rayleigh Number} < 10^7$.

From the experimental results two correlations were developed in terms of Nusselt number and Rayleigh number. These correlations satisfy all of the experimental data within reasonable accuracy.

LIST OF SYMBOLS

Symbol	Meaning	Units
A	Heat Transfer Area	m ²
b	Mean fin spacing	m
c	Thermal capacitance	J/K
g	Gravitational acceleration	m/s ²
h	Convective heat transfer coefficient	W/m ² K
H	Fin height	m
I	Current	Amp
k	Thermal conductivity of air at film temperature	W/m ^o K
L	Fin length	m
Nu	Nusselt number for convection	
p*	ρ/ρ_w^2	
Pr	Prandtl number = ν/α	
Q	Heat	W
Ra	Rayleigh number = $g\beta\Delta T_b^4/\alpha\nu L$	
s	Spacing between fins at base plate	m
t	Width of fin at its base	m
T	Temperature	K
T _b	Surface temperature of the array	
T _F	Film temperature = $T_a + .62 (\bar{T}_{b'} - T_a)$	K
ΔT	$\bar{T}_{b'} - T_a$	K
u, v, w	Velocity components in x,y,z directions	m ² /s
u*, v*, w*	Nondimensional velocities = $\frac{u}{v_o}, \frac{v}{v_o}, \frac{w}{w'}$	
v _o	$\sqrt{g\beta\Delta TL / (1 + Pr)} \cdot \frac{b}{L}$	
w'	$\sqrt{g\beta\Delta TL / (1 + Pr)}$	
V	Voltage	volt
w _o	Approach velocity	m/s
x,y,z	Cartesian coordinates	m
x*, y*, z*	Non-dimensional coordinates = x/b, y/b, z/l	
∞	Thermal diffusivity at film temperature	m ² /s
β	Thermal expansion coefficient at film temperature	1/K
ϵ	Emissivity	

θ	$(T-T_a)/(\bar{T}_b - T_a)$	
ν	Kinematic viscosity at film temperature	m^2/s
ρ	Fluid density at film temperature	kg/m^3
σ	Boltsman constant = 5.6690×10^{-8}	w/m^2K^4

Subscripts

a	ambient
b	Mean fin spacing
conv	Convection
cond	Conduction
f	fin
F	Film temperature
l	loss from the back of the specimen
L	Length of the plate or fin arrays
o	optimum
rad	Radiation
s	Total surface over the finned and unfinned that is exposed in air
Tot	Total

Superscripts

-	Local value/ true value/ average value
*	Nondimensional

CONTENTS

Title	Page No.
CERTIFICATE OF APPROVAL	I
DECLARATION OF THE CANDIDATE	II
CERTIFICATE OF RESEARCH	III
ACKNOWLEDGEMENTS	IV
ABSTRACT	V
LIST OF SYMBOLS	VI
CONTENTS	VIII
CHAPTER 1 INTRODUCTION	1
1.1 General	1
1.1a Extended Surfaces	2
1.1b Compact Heat Exchanger Surfaces	2
1.1c Electrical and Electronic Cooling	3
1.2 Present Work Selection	3
1.3 Objective of the Present Work	3
CHAPTER 2 LITERATURE REVIEW	4
CHAPTER 3 MATHEMATICAL MODELING OF THE PROBLEM	6
3.1 The Governing Differential Equations	6
3.2 Description of the Problem in the Present Work	8
3.3 Mathematical Equation for Correction	9
CHAPTER 4 EXPERIMENTAL SET-UP AND PROCEDURE	11
4.1 Experimental Set-up	11
4.2 Procedure	12

CHAPTER 5	RESULTS AND DISCUSSIONS	14
CHAPTER 6	CONCLUSION AND RECOMMENDATION FOR FUTURE WORK	16
6.1	Conclusion	16
6.2	Recommendation for Future Work	16
REFERENCES		17
APPENDICES		20



CHAPTER-1

INTRODUCTION

1.1 GENERAL

The science of “heat transfer” seeks to explain and predict the process of energy transfer which may take place between material’s bodies as a result of temperature difference. The physical processes involved in the generation and utilization of heat has great many practical importance. Areas of study range from atmospheric and environmental problems to those in manufacturing systems and space research.

There are three basic processes of thermal energy transport: (i) conduction, (ii) convection and (iii) radiation.

(i) Conduction: Conduction occurs if a temperature difference exists in a material and is due to the motion of microscopic particles that comprise the material. The motion of the particles is dependent on local temperature in the material and the energy diffusion is due to differences in motion.

(ii) Convection: In convection, heat transfer processes take place with the motion of the fluid. As a consequence of this fluid motion, the heat transfer rate, as given by conduction is considerably altered.

Convection is inevitably coupled with the conductive mechanism, since, though the fluid motion modifies the transport process, the eventual transfer of energy from one fluid element to another in its neighborhood is through conduction. Also, at the surface, the process is predominantly conduction due to the relative fluid motion being brought to zero at the surface.

The convection heat transfer is divided into two basic processes: (a) forced convection and (b) free convection.

(a) Forced Convection: if the fluid motion arises due to an external agent, such as the externally imposed flow of a fluid stream by a fan, a blower, the wind, or the motion of the heated object itself over a heated object, the process is termed as forced convection.

(b) Free Convection: If there is no internally induced flow is provided and the flow arises "naturally" simply due to the effect of a density difference, resulting from a temperature or concentration difference, in a body force field, such as gravitational field, the process is termed as "natural" or "free" convection. The density difference gives rise to buoyancy effects due to which the flow is generated.

(iii) Radiation: The energy transfer in the last mode in the form of electromagnetic waves is called "radiation". Energy is emitted from a material due to its temperature level, being larger for higher temperature, and is then transmitted to another surface through the intervening space, which may be vacuum or a medium which may absorb, reflect or transmit the radiation depending on the nature and extent of the medium.

1.1a Extended Surfaces

A growing number of engineering disciplines are concerned with energy transitions requiring the rapid movement of heat. They produce an expanding demand for high-performance heat-transfer components with progressively smaller weights, volumes, costs, or accommodating shapes. Extended surface heat transfer is the study of high-performance heat-transfer components with respect to these parameters and of their behavior in a variety of thermal environments. Typical components are found in air-land-space vehicles and their power sources; chemical, refrigeration, and cryogenic processes; electric and electronic circuitry; conventional furnaces and gas turbines; process heat dissipaters and waste-heat boilers; nuclear-fuel modules, direct energy conversion, and many more.

In the design and construction of various types of heat-transfer equipment, simple shapes such as cylinders, bars, and plates are used to implement the flow of heat between a source and a sink. They provide heat-absorbing or heat-rejecting surface, and each is known as a prime surface. When a prime surface is extended by appendages intimately connected with it, such as the metal tapes and spines on the tubes, the additional surface is known as extended surface. Some typical examples of extended surfaces are shown in Fig. 25.

1.1b Compact Heat Exchanger Surfaces

More recently the demands of aircraft, aerospace, gas-turbine, air-conditioning and cryogenic auxiliaries have places particular emphasis on the compactness of heat transfer surface and particularly on those surface elements which induce small pressure gradients in the fluids circulated through them. Several compact heat exchanger surfaces are shown in Fig. 26. Compactness refers to the ratio of heat transfer surface per unit of exchanger volume.

1.1c Electrical and Electronic Cooling

The widespread acceptance of natural convection cooled mainframe computers, extensive array of transistor heat sinks, transistor coolers and the continuing rise in component heat dissipation has spurred extensive research and development of advanced thermal control techniques for electrical and microelectronics.

Natural convection cooling is of interest in the thermal management of different electronic components. These components may be encountered individually, distributed on a single substrate or printed circuit board, or in arrays of vertically-oriented substrates or printed circuit boards. Electronic cooler is shown in Fig. 27a. Natural convection heat transfer is also applied in transistor heat sinks, transistor coolers etc. Some typical transistor heat sinks and transistor coolers are shown in Fig. 27b and Fig. 27c respectively.

1.2 PRESENT WORK SELECTION

The works accomplished in the area of natural convection heat transfer from the fins or fins arrays has increased over five folds in the last 20 years. Natural convection heat transfer find important applications in the cooling of small energy conversion devices, in room air heating and for special heat exchange conditions where trouble-free and noiseless operation are desired. Although a lot of investigations have been conducted with fin/ fin arrays of different profiles, but very little attention has been paid to study the heat transfer behaviour from arrays of triangular fins. Considering the above the present work has been selected for further study.

1.3 OBJECTIVE OF THE PRESENT WORK

The main objectives of this study were as follows:

- i. To design an experimental set-up for studying the natural convection heat transfer from vertical triangular fin arrays.
- ii. To study the effect of temperature on emissivity for different fin arrays.
- iii. To study the effect of radiation heat loss on convection heat loss for different fin arrays.
- iv. To examine the natural convection heat transfer rate from triangular fin arrays at vertical orientation.
- v. To develop a correlation for estimation of natural convection heat transfer from four-type of fin arrays.
- vi. To establish the effect of number of fins in an array on heat transfer enhancement.
- vii. To compare the results of this study with other relevant works.

CHAPTER-2

LITERATURE REVIEW

Heat transfer from fins is a topic of continuing interest in heat transfer. Although in practice the rectangle has been the most common fin shape but the triangular fins have a higher rate of heat transfer per unit of material volume; indeed, by this measure, its performance approaches quite closely that of the optimal shape which is explained in Appendix-C1. The common practice of using rectangular fins would seem to stem from the difficulty of manufacturing other shapes, particularly when the fins are fabricated from sheet metal. When the fins are extruded, however, they are more often triangular. This is often the case even when rectangular fins were intended, because of limitations in the extrusion process.

To design a fin properly one needs to know the convective heat transfer coefficient to the surrounding fluid. Interestingly, it appears that very few measurements have been reported in the literature of the natural convective heat transfer coefficients from triangular fins mounted in a vertical surface, which is the most common orientation.

Several researchers have studied heat transfer rate from different fin profile. Harper and Brown [2] studied the temperature gradient along the length and efficiency of straight fins of rectangular, triangular & trapezoidal profile and circular fins of rectangular profile. Later Schmidt [3] investigated straight and circular fins from the point of least-lateral requirements for which the temperature gradient is linear. Avrami and Little [4] have studied the temperature gradients dt/dx and dt/dh in thick fins of rectangular profile and have established the critical Nusselt number below which straight rectangular fins are useful.

Gardener [5] has generalized the extended surface problem by deriving general equations for the efficiency from the generalized Bessel's equation. Zabronsky [6] has presented an exact solution for the efficiency of square fins on round tubes. Elenbaas, 1942 [7]; Starner and McManus, 1963 [8]; Willing and Wooldridge, 1965 [9]; Schult, 1966[10]; Aihara, 1970 [11]; Chaddock, 1970 [12] have also studied heat transfer for vertical rectangular fins. Works of different prominent scientists are described in Appendix-C2. And equations of review works are listed in Table-B.

It seems likely that designers (Karagiozis [13], Elenbaas [7]) of triangular fins have used recommended equations to calculate heat transfer from the triangular fins assuming, for example, that the triangular fin will convect the same as a rectangular fin of the same perimeter facing a passage of the same cross-sectional area.

Raithby and Hollands' work [13] is on the basis of above mentioned procedure. They studied natural convection heat transfer from arrays of triangular fins by applying transient method. They used aluminum 2024-T35 and 6061-T6 as base plate and the fins were bolted to the base plates and good thermal contact was obtained by placing a strip of aluminum foil smeared with vacuum grease between the fin and base plate. But in the present work cast iron was used as base plate as because of it's availability and low cost, and the fins were the integrated part of the base plate to minimize the surface contact resistance.

A triangular fin would have less boundary layer interference near its tips and more boundary layer interference near its base. Also, heat transfer from the fin ends is going to be different for above mentioned two cases. Even if the rectangular fins and triangular fins did dissipate heat at the same rate, there would still be a problem. For vertical rectangular fins there are substantial differences between the recommended equations of different researchers (Chaddock [12], Elenbaas [7]) is most pronounced at low Rayleigh numbers. The reason is that the corrections for the radiant losses and for the back losses become relatively large at low Rayleigh number, and there is usually a large uncertainty in both of these corrections. In the present measurements, every effort was made to minimize the radiant and back losses.

CHAPTER-3

MATHEMATICAL MODELING OF THE PROBLEM

3.1 THE GOVERNING DIFFERENTIAL EQUATION

If Q_{conv} is the convective heat transfer to the ambient fluid from the surface area A_s , the average heat transfer coefficient is embodied in the Nusselt number as follows:

$$N_u = \frac{\bar{h}b}{k} = \frac{Q_{\text{conv}}b}{A_s\Delta T k}$$

The parameters upon which Nu depends are obtained by a dimensional analysis. By retaining only the terms in the governing equations that are important for natural convection and neglecting property value variations, the non-dimensional equations of continuity, momentum and energy, for the vertical fin arrays in Fig. 21 can be expressed by

$$\text{Continuity: } \frac{\partial u^*}{\partial x^*} + \frac{\partial v^*}{\partial y^*} + \frac{\partial w^*}{\partial z^*} = 0; \quad [1a]$$

$$\begin{aligned} \text{Momentum: } u^* \frac{\partial u^*}{\partial x^*} + v^* \frac{\partial u^*}{\partial y^*} + w^* \frac{\partial u^*}{\partial z^*} &= -\left(\frac{L}{b}\right)^2 \frac{\partial p^*}{\partial x^*} \\ &+ \sqrt{\text{Pr} \frac{(1+\text{Pr})}{\text{Ra}}} \left(\frac{\partial^2 u^*}{\partial x^{*2}} + \frac{\partial^2 u^*}{\partial y^{*2}} + \frac{b^2}{L^2} \frac{\partial^2 u^*}{\partial z^{*2}} \right); \end{aligned} \quad [1b]$$

$$\begin{aligned} u^* \frac{\partial w^*}{\partial x^*} + v^* \frac{\partial w^*}{\partial y^*} + w^* \frac{\partial w^*}{\partial z^*} &= -\frac{\partial p^*}{\partial z^*} \\ &+ \sqrt{\text{Pr} \frac{(1+\text{Pr})}{\text{Ra}}} \left(\frac{\partial^2 w^*}{\partial x^{*2}} + \frac{\partial^2 w^*}{\partial y^{*2}} + \frac{b^2}{L^2} \frac{\partial^2 w^*}{\partial z^{*2}} \right) \end{aligned} \quad [1c]$$

$$\text{Energy: } u^* \frac{\partial \theta}{\partial x^*} + v^* \frac{\partial \theta}{\partial y^*} + w^* \frac{\partial \theta}{\partial z^*} = (1 + \text{Pr})\theta + \sqrt{\frac{\text{Pr}(1 + \text{Pr})}{\text{RaPr}}} \left(\frac{\partial^2 \theta}{\partial x^{*2}} + \frac{\partial^2 \theta}{\partial y^{*2}} + \frac{b^2}{L^2} \frac{\partial^2 \theta}{\partial z^{*2}} \right) \quad [1d]$$

$$\text{Ra} = \frac{g\beta\Delta T(b^4/L)}{\nu\alpha} \quad [1e]$$

The v^* momentum equation has not been written since it is exactly the same as Eq. [1b] with the dependent variable u^* replaced by v^* . The coordinates are shown in Fig. 8, and the dimensionless variables are defined in the nomenclature. It should be noted in deriving these equations the length and velocity scales used in the vertical direction are different from those in the horizontal direction. The Rayleigh number based on the length scale in Eq. [1e] is often referred to as the Elenbaas Rayleigh number.

The boundary conditions must still be recorded, and examined for additional dimensionless groups. On the fin surface the boundary conditions are

$$\theta = \frac{T - T_a}{T_b - T_a} = 1$$

$$u^* = v^* = w^* = 0, \quad \theta = 1$$

When the fin surface is plotted in (x^*, y^*, z^*) coordinates, a fin array will be coincident if the ratio H/b , t/b , W/b and t_{base}/b are identical, it is important to note that L/b does not appear in this list because, by the definition $z^* = z/L$, all fin surfaces lie in the range $0 \leq z^* \leq 1$.

G. D. Raithby and K. G. T. Hollands [13] have expressed Nu as follows.

$$Nu = f\left(Gr, Pr, \frac{L}{b}, \frac{H}{b}, \frac{t}{b}, \frac{W}{b}, \frac{t_{\text{base}}}{b}, \frac{R_0}{b}, \frac{\beta gb}{C_p}\right)$$

- For non enclosure effects, $R_0 \rightarrow \alpha$.
- $t_{\text{base}} \rightarrow 0$ as $A_{\text{base}}/A_s \ll 1$.
- $Nu = f_{\Delta^*}[\Delta^* \theta]_s \cdot \hat{n} dA_s^*$; $\Delta^* \theta = \frac{\partial \theta}{\partial x^*} \hat{i} + \frac{\partial \theta}{\partial y^*} \hat{j} + \frac{b}{L} \frac{\partial \theta}{\partial z^*} \hat{k}$

$[\Delta^*\theta]$ is non-dimensional gradient, \hat{n} is unit surface normal, A^*_s is non-dimensional surface area]

In vertical surface (i.e. $\hat{n} \cdot \hat{k} = 0$) there is no effect of L/b .

- $\beta gb/C_p$ is a frictional heating. Ostrach [22] showed that

$$Nu = \left(Gr.Pr. \frac{\beta gb}{C_p} \right) = f(k), \text{ frictional heating is important when } k = 10. \text{ But in the}$$

present work $k = 0.1$. So, $\beta gb/C_p$ can be neglected.

- For large number of fins $W/b \gg 1$, i.e., W/b can be neglected.
- For large Ra , heat transfer becomes independent of fin shapes. When Ra is sufficiently high, the boundary layers to be much smaller than the fin spacing, each vertical strip of the fin array will transfer the same heat as any other strip and at high value of Ra , heat transfer from bottom and top ends can be neglected. So fin shape ratio H/b , t/b can be neglected. So the final form of Nusselt number becomes:

$$\therefore Nu = f(Gr.Pr.) = f(Ra) \quad [1f]$$

3.2 DESCRIPTION OF THE PROBLEM IN THE PRESENT WORK

The objective was to measure the convective heat transfer, Q_{conv} . If Q_{conv} is the convective heat transfer to the ambient fluid from the surface area A_s , where A_s is the entire surface area of the array except the back and side (Fig. 21), the average heat transfer coefficient is embodied in the Nusselt number as follows:

$$Nu_b = \frac{\bar{h}b}{k} = \frac{Q_{conv}b}{A_s \Delta T k} \quad [2a]$$

The parameters on which Nu depends are obtained by a dimensional analysis which has been discussed above.

Nu numbers should be applicable to all geometrically similar arrays, for the same Ra and Pr . To measure the total heat loss from the fin arrays, a steady state technique was used. Heat loss consists of three components and heat balance from the specimen's surface becomes:

$$Q_{Total} = Q_{conv} + Q_{rad} + Q_i \quad [2b]$$

where Q_{rad} is the radiation loss and Q_i is the loss from the back of fin base.

Q_{conv} can be found by subtracting Q_{rad} and Q_l . Raithby and Holland's [13] method was used to measure the Q_{rad} .

$$Q_{rad} = \sigma A_s F_{1-2} (\bar{T}_b^4 - T_a^4) \quad [2c]$$

where the radiant exchange factor F_{1-2} (Krieth, 1968) accounts for both geometric and surface emissivity effects governing radiant exchange between the fins and the surroundings. The value of F_{1-2} equals to ϵ as the area A_s is very small with respect to room.

Final form of the governing equation becomes:

$$\begin{aligned} Q_{conv} &= Q_{Total} - Q_{rad} - Q_l \\ \Rightarrow Q_{conv} &= Q_{Total} - \sigma A_s \epsilon (\bar{T}_b^4 - T_a^4) \end{aligned} \quad [2d]$$

[$\therefore Q_l = \text{negligible}$]

3.3 MATHEMATICAL EQUATIONS FOR CORRECTION

3.3a Corrected Equation for Convective Heat Transfer

The objective was to measure the convective heat transfer, Q_{conv} , so that Nu can be calculated, as

$$Nu_b = \frac{Q_{conv} b}{A_s \Delta T k}$$

Though $h = Q_{conv}/A_s \Delta T$, but h should be corrected by \bar{h} . S.M. Dusenberre (24) has introduced an equation for triangular fin efficiency, $\theta = 1/(1+hH^2/kt)$.

Again,

$$\begin{aligned} h &= [A_{b'}(\bar{T}_{b'} - T_a) + A_f\theta(\bar{T}_{b'} - T_a)] = \bar{h}A_s(\bar{T}_{b'} - T_a) \\ \Rightarrow \bar{h} &= h = [x + \theta(1-x)] \end{aligned} \quad [3a]$$

where, $x = A_{b'}/A_s$, $A_{b'} + A_f = A_s$.

Therefore, corrected Q_{conv} is

$$Q_{\text{conv}} = \bar{h}A_s\Delta T \quad [3b]$$

3.3b Corrected Equation for Film Temperature

The physical properties used in the calculation of Nusselt and Rayleigh numbers were evaluated at a “film Temperature” of

$$T_F = T_a + 0.62(\bar{T}_{b'} - T_a) \quad [3c]$$

as recommended by Sparrow and Gregg [23].

CHAPTER-4

EXPERIMENTAL SET-UP AND PROCEDURE

4.1 EXPERIMENTAL SET-UP

The set up consists of test bench, test section and measuring instruments. The sketch of the set up is shown in Fig. 22.

a. The Test Bench

The test bench was fabricated from mild steel angle frame. It has two parts. In one part the test section might be installed. The other part is moveable. The test bench was mounted on a trolley.

b. The Test Section

The test section consists of specimen (fin array) and heater. All the specimens were prepared by sand casting. After casting the specimens were cooled in air to ambient temperature and were machined by a shapper. The specimens were painted black-mat and were attached with a mild steel plate installed in the test bench. A sketch of the specimens is shown in Fig. 21. The dimensions of the specimen are listed in the Table-A. A 100 watt electric heater made of 28 BWG nicrome wire was mounted on the back portion of cast iron base plate of fin array. Back portion of the test section was insulated by asbestos sheet to minimize the heat losses. The test section is shown in Fig. 23.

c. Measuring Instruments

The set up was instrumented by a stabilizer, a voltage regulator, an ammeter, a voltmeter, an infrared thermometer, and a digital thermometer.

Digital Thermometer

A digital thermometer was used to measure the temperature of the fin surface and that of the ambient air. The thermometer was a high precision one. It could measure the temperature upto 0.1°C.

Five thermocouples were embedded in 8 mm deep holes in the base plate, another three were attached on the fin surface and one thermocouple was used to measure the temperature of the surrounding air. The iron constantan thermocouples (J-type) were used in this experiment. The positions of the thermocouples are shown in Fig. 23. All the thermocouples were calibrated.

Non-Contact Infrared Thermometer (NCIT)

The contribution of radiation heat transfer in natural convection is quite significant. So in this experiment a non-contact infrared thermometer was used to estimate the emissivity of the fin surface. After knowing the emissivity the heat loss from the specimen by radiant mode was calculated. The specifications of non-contact infrared thermometer is mentioned in the Appendix-E. The parts name and functions of the non-contact infrared thermometer is shown in Fig. 24. The main components of the non-contact infrared thermometer are its body and a probe.

The probe contains lens to read out the infrared radiation from the specimen. To get the better result, the specimen must be at least 1.5 times the spot size (spot diameter = 10 mm) and the probe must be held horizontally facing the specimen for more than 20 minutes at a distance of 5 cm from the specimen.

Emissivity Measurement Technique

At first an approximate reasonable value of emissivity of the specimen was assumed. The value of the emissivity was set by emissivity key of the NCIT. The following operation is to be carried out when setting the emissivity not to the initial value ("1.00") but to a value specific to the specimen to be measured.

- i. The power switch is to be OFF and ON again, or to be displayed "ε" by the MODE key.
- ii. The emissivity value should be altered by the ∇ or Δ keys. The value is to be altered continuously by keeping ∇ or Δ keys pressed down.

The emissivity was set in such a way that the temperature of the specimen was identical to the NCIT read out "average fin surface temperature". The emissivity obtained against the average fin surface temperature was the emissivity of the specimen.

4.2 PROCEDURE

The investigations were carried out with four different test specimens having varied number of fins in the array. The specimens were: (a) a flat plate with single triangular fin, (b) an array of four triangular fins, (c) an array of seven triangular fins and (d) an array of thirteen triangular fins. The total number of test runs were around fifty.

At the beginning of the test run the natural convection heat transfer from a flat plate was performed in order to compare the results obtained from a single fin and fin arrays. The experiments were performed in a draft free room. A brief outline of the experimental procedure is given below:

- i. The specimen was firmly mounted in the test bench.
- ii. The heater was switched on to heat the specimen.
- iii. After attaining the steady state (generally it took 2 to 3 hours to attain the steady-state) all the readings (base plate temperature, ambient temperature, voltmeter, ammeter, etc.) were noted.
- iv. Using the procedure (described in the section 4.1) the emissivity of the specimen was measured by a non-contact infrared thermometer.

In each run input power of the electric heater was cross-checked using a multimeter by measuring the resistance of the heater and input current.

CHAPTER-5

RESULTS AND DISCUSSIONS

Investigations were carried out for natural convection heat transfer from different triangular fin arrays. The experimental data (heat input, prime surface and fin surface temperature, ambient temperature, emissivity, etc.) are given in the table 1-8. The outcome of the experiments were expressed by dimensionless group, Nusselt & Rayleigh number and was incorporated in the above mentioned table .

Fig. 10 represents the experimental measurement of emissivity for different fin arrays. The emissivity of the fin arrays increases with the increase of fin surface temperature. At a definite temperature emissivity of the fin arrays increases with the increase of number of fin in the array. The results of the emissivity shows that there is no variation of emissivity in between 4 fin and 7 fin array at a definite temperature.

Fig. 11a to 11c show the comparison of radiation and convection heat transfer from fin arrays. In this experiment, the radiative heat transfer, Q_{rad} was calculated using Equation (2c). Q_{rad} was used to calculate “radiation Nusselt number” Nu_{rad} where Q_{conv} in Equation (2a) is replaced by Q_{rad} . It is clear from this figure that failure to account the radiation will result a severe underestimation of the heat loss from the fin surface.

Fig. 12 shows the comparison of natural convection heat transfer between the present work and that of Eckert & Drake [15] for vertical flat plate. The experimental data shows a good agreement.

Fig. 13, 14, 15 & 16 show the comparison of natural convection heat transfer between the present work with that of Hassani-Holland's equation [21]. From the above Figs. it is observed that the generated data fully conforms with that of the Hassani-Holland's equation, which is generally recommended for natural convection heat transfer from three dimensional bodies of irregular geometry oriented in arbitrary directions.

The heat transfer augmentation with the increase of total heat flux for different fin array is depicted in Fig. 17a. The Fig. 17a shows that natural convection heat transfer increases with the increase of number of fin in the array.

Fig. 17b depicts the results of natural convection heat transfer from different fin arrays. The results obtained from the generated data were also compared with that of a single fin and flat plate. From Fig. 17b it is evident that for an array consists of 13 fins, Nu number increases approximately at a constant rate with the increase of Rayleigh number from 0.439 to 9.714. For an array consists of 7 fins, Nu number increases approximately at a constant rate with the increase of Rayleigh number from 47.8 to 344.7. And for an array consists of 4 fins, Nu number increases approximately at a constant rate with the increase of Rayleigh number from 340 to 3991.

In Fig. 18 all the generated data were replotted. After analysing this figure it is evident that for $Ra \geq 10^4$, all the arrays merges into a single curve. At lower Ra experimental data indicates that heat transfer rate is almost independent of Ra as the curve becomes almost horizontal.

From the experimental data of this work the following correlation may be obtained for Rayleigh number $\geq 10^4$:

$$Nu_L - 3.254 = 0.515Ra^{1/4}; \quad Ra \geq 10^4 \quad (4a)$$

The measured Nu values are best fit by the above equation. The datas that were plotted does not deviate more than 3.7 percent.

Analysing the Fig. 18, for the generated experimental data, the following correlation may be recommended:

$$Nu_L - 0.779 = 0.515Ra^{1/4} \left(1 + \left(\frac{3.26}{Ra^{0.21}} \right)^3 \right)^{-1/3}; \quad 10^{-1} < Ra \leq 10^4 \quad (4b)$$

The measured Nu values are best fit by the above equation. The datas that were plotted deviates not more than 1.6 percent.

The effect of fin population on convective heat transfer is depicted in Fig. 19. It is observed that the experimental parameters Nu number increases with the increase of number of fins in an array at a definite Rayleigh number.

Fig. 20 shows the comparison of experimental datas with the equation of vertical flat plate by Eckert and Drake [15], vertical triangular fin arrays by Raithby and Holland [13] and vertical rectangular fin arrays by Chaddock [20]. Analysing Fig. 20 it is observed that for the identical condition triangular fin arrays enhance heat transfer more than the rectangular fin arrays.

CHAPTER-6

CONCLUSIONS AND RECOMMENDATION FOR FUTURE WORK

6.1 CONCLUSIONS

The present work reports the measurements of natural convective heat transfer from triangular fin arrays to ambient air. The important conclusions as a consequence of the present investigation are enumerated below:

- i. The investigations revealed that the use of fin arrays provide better results only upto Rayleigh number less than or equals to 10^4 , beyond that fin arrays does not enhance the heat transfer.
- ii. For Rayleigh number grater than or equals to 10^4 , the following correlation may be used in estimating the natural convection heat transfer from triangular fin arrays.

$$Nu_L - 3.25 = 0.515Ra^{1/4}$$

- iii. For Rayleigh number from 0.1 to 10^4 , the following correlation may be used:

$$Nu_L - 0.779 = 0.515Ra^{1/4} \left[1 + \left(\frac{3.26}{Ra^{0.21}} \right)^3 \right]^{-1/3} ; 10^{-1} < Ra \leq 10^4$$

6.2 RECOMMENDATION FOR FUTURE WORK

The following recommendations are put forward as a future improvement of the present investigations:

- i. Further investigations can be carried out in order to determine the optimum dimension of fin in the array.
- ii. The entire investigation can also be repeated with fin arrays of different materials, such as, brass, copper, aluminum, mild steel, etc.
- iii. A series of experiments can be carried out in order to elucidate the heat transfer behaviour between fins arrays with its surrounding.
- iv. Natural convection heat transfer from fin arrays may be carried out at different angle of inclination, such as 10° , 30° , 50° , 70° from the horizontal.

REFERENCES

1. **Eckert, E.R.G. and Drake, R.M.**, "Analysis of Heat and Mass Transfer", McGraw-Hill, Ny, 1972, pp. 89-90.
2. **W.B. Harper, and D.R. Brown**, "Mathematical Equations for Heat Conduction in the Fins of Air-Cooled Engines", NACA Report No. 158, Washington; 1922, pp. 679-708.
3. **E. Schmidt**, "Die Wärmeübertragung Durch Rippen", Zeit, VDI, Vol. 70, 1926, pp. 885-889, 947-951.
4. **M. Avrami, and J.B. Little**, "Diffusion of Heat Through a Rectangular Bar and the Cooling and Insulating Effect of Fins", Journal of Applied Physics, Vol. 13, 1942, pp. 255-264.
5. **K. A. Gardner**, "Efficiency of Extended Surface", Trans. ASME, Vol. 67, No. 8, 1945, pp. 621-631.
6. **H. Zabronsky**, "Efficiency of a Heat Exchanger Using Fins on Round Tubes", USAEC, K-929, Oak Ridge Technical Information Service, August, 1952, (ASME Reprint No. 54-A-12).
7. **W. Elenbaas**, "Heat Dissipation of Parallel Plates by Free Convection", Rep. Physica, Vol. IX, 1942, pp. 1-28.
8. **K.E. Starner and H.N. Mcmanus**, 1963, "An Experimental Investigation of Free Convection Transfer From Rectangular Fin Arrays", ASME Journal of Heat Transfer, Vol. 85, pp. 273-278.
9. **J. R. Welling and C. B. Wooldridge**, "Free Convection Heat Transfer Coefficients from Rectangular Vertical Fins", ASME Journal of Heat Transfer, Vol. 87, 1965, pp. 439-444.
10. **T. H. Schult**, "Free Convection Heat Transfer From Rectangular Fin Arrays", M.S. Thesis, Mechanical Engineering Department, Purdue University, W. Lafayette, IN.

11. **T. Aihara, 1970a** "Natural Convection Heat Transfer From Vertical Rectangular-fin Arrays Part-1", Rep. Inst. High Sp. Mech., Japan, Vol. 21, No. 213, 1970a, pp. 105-134.
12. **J. B. Chaddock, 1970**, "Free Convection Heat From Vertical Rectangular Fin Arrays", ASHRAE Journal, Vol. 12, August, 1970, pp. 53-60.
13. **A. Karagiozis, G. D. Raithby and K.G.T. Hollands, 1994**, "Natural Convection Heat Transfer From Arrays of Isothermal Triangular Fins in Air", Journal of Heat Transfer, Vol. 116/105.
14. **J.D. Hellums, and S.W. Churchill**, "Dimensional Analysis and Natural Convection, Chemical Engineering Progress Symposium Series", Vol. 57, No. 32, 1961.
15. **E.R.G. Eckert and R.M. Drake**, "Heat and Mass Transfer", McGraw-Hill Book Co., New York, 1959, pp. 47 & 315.
16. **Ostrach**, "Completely Confined Natural Convection. Developments in Mechanics", 4, Proc. of 10th Midwestern Mechanics Conference", Johnson Pub. Co., 1968, pp. 53-81.
17. **J. R. Bodoia and J. F. Osterle**, "The Development of Free Convection Between Heated Vertical Plates", Trans. ASME. Series C. Jour. Heat Transfer, vol. 84, 1962, pp. 40-44.
18. **W. Elenbaas**, "Heat Dissipation of Parallel Plates by Free Convection", Physica, Vol. IX, 1942, pp. 1-28.
19. **W. Elenbaas**, "Dissipation of Heat by Free Convection", Phillips research Report, Part-I, Vol. 3, 1948, pp. 338-360; Part-II, Vol. 3, 1948, pp. 450-465.
20. **J. A. Edward and J. B. Chaddock**, "Free Convection and Radiation Heat Transfer from Fin-on-Tube Heat Exchanges", ASME Paper 62WA 205..

21. **A. V. Hassani and K.G.T. Hollands**, "On Natural Convection Heat Transfer From Three-Dimensional Bodies of Arbitrary Shape". Journal of Heat Transfer, May 1989, Vol. 111/363.
22. **S. Ostrach**, "Laminar Natural Convection Flow and Heat Transfer of Fluids with and without Heat Sources in Channels with constant Wall Temperature", NACA Tech. Note 2863, 1952.
23. **E.M. Sparrow and J. L. Gregg**, "The Variable Fluid-Property Problem in Free Convection", Trans. ASME, 80, Nov. 1945, pp. 621-631.
24. **G. M. Dusinberre**, "Effective and Local Surface Coefficients in Fin Systems", Trans. ASME, Vol. 80, 1958, pp. 1596-1597.
25. **Kline and McClintock, 1953**, "Uncertainties in Single-Sample Experiments", January 1953, ASME.
26. **P. J. Schneider**, "Conduction Heat Transfer", 1955, 3rd Edition.
27. **Park, K. A. and Bergles, A. E.**, "Natural Convection Heat Transfer Characteristics of Simulated Microelectronic Chips", J. of Heat Transfer, Vol. 109, 1987, p. 90.
28. **Baker, E.**, "Liquid Cooling of Microelectronic Devices by Free and Forced Convection, Microelectronics and Reliability", Vol. 11, 1972, p.213.
29. **Bar-Cohen, A. and Schweitzer, H.**, "Convective Immersion Cooling of Parallel Vertical Plates, IEEE CHMT Transactions", Vol. 8, No. 3, 1985, p.343.
30. **Y. M. S. Ibrahim and A. A. Badran**, "Heat Transfer in External Stone Wall; the Effect of Stone Surface Texture"; Proceeding of the 2nd Jordanian International Conference for Mechanical Engineering, JIMEC-97, Held at Amman, Jordan 1-5 January, 1997, p. 351-380.
31. **Bhavani, S. H. and Bergless, A. E.**, "An Experimental Study of Laminar Natural convection Heat Transfer from Wavy Surfaces", ASME Transfer, Vol. 96, pp. 173-180, (1988).

APPENDIX-A: SAMPLE CALCULATION

SAMPLE CALCULATION OF FIN ARRAYS

Nu_b (Hassani & Holland's [21] equation):

$$A_s = A_b + A_f + A_{\text{Fin bottom}} = 0.023643 + 0.121358 + 0.0042 = 0.1492 \text{ m}^2$$

$$Ah = 0.0021 \text{ m}^2$$

$$N^3 = 0.0987,$$

$$N = 0.4622$$

$$\bar{p} = 0.681 \text{ m}$$

$$\bar{c}_1 = 0.10486$$

$$\hat{c}_1 = 0.0876$$

Therefore,
$$Ra_N = \frac{g\beta\Delta TN^3}{\nu\alpha} = 141335592.9$$

$$m = 6.659, \quad n/m = 0.161, \quad n = 1.07, \quad 1/n = 0.9346$$

Therefore, using equation (10a)

$$Nu_{\sqrt{A_s}} = 61.233$$

or, $Nu_b = 3.59$

Experimental Nu_b :

$$VI = Q_{\text{conv}} + \sigma A_s \varepsilon (\bar{T}_b^4 - \bar{T}_a^4)$$

From equation (9b), $\Rightarrow 12.34249 = Q_{\text{conv}} + 5.669 \times 10^{-8} \times 0.63 \times (318.68^4 - 304^4)$

$$\Rightarrow Q_{\text{conv}} = 7.634$$

Now,

$$Nu_b = \frac{Q_{\text{conv}} \cdot b}{A_s \Delta T k} = 3.227$$

$$\Rightarrow Nu_b = 3.227$$

APPENDIX-B: TABLE

Table-1: Vertical Flat Plate.

Sl. No.	$Q_{Tot} = VI$	$\bar{T}_{b'}$	T_a	T_F	ΔT	Ra_L	Nu_L (Experimental)	Nu_L (Eckert & Drake equation)
1	.621	33	31.0	32.544	2.0	1.0239×10^6	14.950	17.38
2	1.0768	34.4571	31.3	33.2574	3.1571	2.6630×10^6	18.328	22.084
3	1.8599	35.8714	31.0	34.0222	4.87	4.0578×10^6	22.66	24.535
4	3.07734	40.6714	32.0	37.3763	8.6714	6.85×10^6	24.28	27.967
5	4.655	45.8429	31.3	40.5429	14.5429	1.0973×10^6	25.54	31.46

Graph of Table-1 is shown in Fig. No. 12.

Table-2: Vertical Flat Plate with Single Fin.

Sl. No.	$Q_{Tot} = VI$	$\bar{T}_{b'}$	T_a	T_F	ΔT	Ra_L	Nu_L (Experimental)	Nu_L (Hassani & Holland's equation)
1	.039233	31.134	31.0	31.083	0.134	1.49×10^4	4.821	5.41
2	0.57955	31.197	31.0	31.12214	0.197	8.38×10^4	7.35	9.04
3	0.9215	31.4429	31.2	31.351	0.2429	2.1129×10^5	11.88	11.1972
4	.9314	33.3143	31.1	32.4729	2.2143	1.8916×10^6	15.364	17.89
5	2.6678	35.6857	31.4	33.057	4.2857	3.627×10^6	14.91	20.67
6	3.9738	39.7429	31.3	36.5346	8.4429	6.759×10^6	16.46	23.83
7	5.3711	44.7857	32.1	39.965	12.6857	9.624×10^6	17.59	25.423

Graph of Table-2 is shown in Fig. No. 13.

Table-3: Arrays of Four Fins.

Sl. No.	$Q_{Tot} = VI$	$\bar{T}_{b'}$	T_a	T_F	ΔT	Ra_b	Nu_b (Experimental)	Nu_b (Hassani and Holland's equation)	Nu_{rad} (Experimental)
1	.179	31.326	30.9	31.164	.426	3.4×10^2	1.932	2.03	7.59
2	.37889	31.872	31.0	31.541	.872	1.91×10^3	2.625	3.72	7.622
3	.6972	32.3	31.3	31.882	1.0	3.991×10^3	3.32	4.742	7.63
4	1.695	33.2	30.7	32.25	2.5	7.62×10^3	4.25	5.463	7.65
5	2.4637	35.47	31.3	33.886	4.17	1.2379×10^4	5.715	6.115	7.66
6	4.8465	37.3857	30.9	34.92	6.4857	1.89×10^4	6.447	7.218	7.69
7	12.34249	45.6857	31.0	40.105	14.6857	3.9×10^4	7.64	8.5157	7.9

Graph of Table-3 is shown in Fig. No. 14 and 11a.

Table-4: Arrays of Seven-Fin.

Sl. No.	$Q_{Tot} = VI$	$\bar{T}_{b'}$	T_a	T_F	ΔT	Ra_b	Nu_b (Experimental)	Nu_b (Hassani and Holland's equation)	Nu_{rad} (Experimental)
1	0.7008	31.5	30.3	31.044	1.2	4.78×10^1	0.98	1.19	3.27
2	1.1444	32.43	30.5	31.6966	1.93	1.08×10^2	1.2	1.85	3.29
3	1.81285	32.8	30.7	32.002	2.1	2.25×10^2	1.72	2.365	3.29
4	3.21	33.7429	30.5	32.511	3.2429	3.447×10^2	2.354	2.61	3.29
5	7.5312	38.4571	31.3	35.7374	7.1571	7.2265×10^2	2.54	3.065	3.30
6	14.079	42.4857	30.8	38.045	11.6857	1.1378×10^3	3.261	3.376	3.30
7	16.07449	43.8571	30.6	38.8194	13.2571	1.3297×10^3	3.227	3.59	3.32

Graph of Table-4 is shown in Fig. No. 15 and 11b.

Table-5: Thirteen-Fin Arrays.

Sl. No.	$Q_{Tot} = VI$	\bar{T}_b'	T_a	T_F	ΔT	Ra_b	Nu_b (Experimental)	Nu_b (Hassani and Holland's equation)	Nu_{rad} (Experimental)
1	0.0938	31.4212	30.5	31.071144	0.9212	4.39×10^{-1}	0.252	0.387	1.230
2	1.2129	31.934	30.7	31.4651	1.234	1.38×10^0	0.439	0.589	1.231
3	3.01	32.88	30.9	32.13	1.98	2.52	0.690	0.7589	1.232
4	7.1485	35.057	30.6	33.36	4.457	5.556	0.7959	0.9119	1.257
5	13.628	38.79	30.7	35.713	8.09	9.717	0.821	1.038	1.290
6	40.373	47.783	31.0	41.41	16.783	1.844×10^1	1.621	1.7457	1.349

Graph of Table-5 is shown in Fig. No. 16 and 11c.

Table-6: Comparison of Experimental Results with Other Relevant Works.

Sl. No.	Ra_b	Nu_b (Experimental)	Nu_b (Raithby & Hollands' Equation)	Nu_b (Chaddock's Equation)
1	7.08×10^6	19.050	27.08	9.926
2	2.08×10^6	18.650	20.06	7.310
3	8.66×10^4	10.374	9.289	3.280
4	1.49×10^4	7.964	6.073	2.050
5	7.76×10^3	4.999	5.183	1.690
6	7.80×10^2	3.279	2.899	0.652
7	3.49×10^2	1.520	2.343	0.425
8	2.29×10^2	1.293	2.090	0.339
9	1.02×10^2	1.939	1.683	0.220
10	4.76×10^1	1.734	1.382	0.146
11	1.40×10^0	1.200	0.715	0.022

Graph of Table-6 is shown in Fig. No. 20.

Table-7: Demonstration of Fin Population which Yields the Maximum Heat Transfer Rate.

	Ra = 10 ^{1.1}				Ra = 10 ^{1.5}				Ra = 10 ^{2.0}				Ra = 10 ^{2.1}			
Nusselt No.	.7	.8	.9	.95	.8	.9	1	1.10	.9	1	1.1	1.15	1	1.1	1.2	1.25
Fin No. (N)	1	4	7	13	1	4	7	13	1	4	7	13	1	4	7	13

Graph of Table-7 is shown in Fig. No. 19.

Table-8: Effect of Temperature on Emissivity for Different Fin Arrays.

Sl. No.	Single Fin with Flat Plate		Array of 4 Fins		Array of 7 Fins		Array of 13 Fins	
	T _b '	ε	T _b '	ε	T _b '	ε	T _b '	ε
1	31.13	0.57	32.30	0.59	22.80	0.59	32.88	0.68
2	31.19	0.57	33.20	0.594	33.74	0.595	35.05	0.689
3	31.44	0.58	35.47	0.598	38.45	0.60	34.51	0.69
4	33.31	0.59	37.38	0.60	42.48	0.605	38.79	0.696
5	35.68	0.59	45.68	0.61	43.85	0.61	47.78	0.71

Graph of Table-8 is shown in Fig. No. 10.

Table-A: Dimensions of Test Specimens.

	L (m)	W (m)	H (m)	S (m)	b (m)	A _s (m ²)
Flat plate	0.215	0.215	--	--	--	0.0462
Plate with single fin	0.215	0.215	0.0385	--	--	0.0602
4-fin arrays	0.215	0.215	0.04	0.45	0.0525	0.1033
7-fin arrays	0.213	0.216	0.04	0.01566	0.02266	0.1492
13-fin arrays	0.215	0.215	0.04	--	0.0075	0.2225
	t _{base} = 0.010 m			t = 0.015m		

Fin arrays are shown in Fig. 21.

Table-B: Review Works on Different Type of Fin Profile.

Fin Profile Type	Correlations	Author
Straight Rectangular	efficiency = $\frac{1}{\sqrt{2\xi}} \tanh \sqrt{2\xi}$	B. Gebbart [26]
Trapezoidal	efficiency = $\frac{\pi k \eta_2 \tan \theta}{4hH} \left[\frac{I_1(\eta_2)k_1(\eta_1) - I_1(\eta_1)k_1(\eta_2)}{I_0(\eta_2)k_1(\eta_1) - I_1(\eta_1)k_0(\eta_2)} \right]$	B. Gebbart [26]
Triangular	$e = 1/\zeta \times \frac{I_1(2\zeta)}{I_0(2\zeta)}$	B. Gebbart [26]
Inward parabolic	$e = 2 / \left(1 + \sqrt{1 + \frac{8}{3}\xi^2} \right)$	B. Gebbart [26]
Outward parabolic	$e = \frac{1}{\sqrt{4/3\xi}} \cdot \frac{I_{2/3}[(4/3)^{3/2}\xi]}{I_{-1/3}[(4/3)^{3/2}\xi]}$	B. Gebbart [26]
Vertical flat plate	$Nu_x = 0.508 Pr^{1/4} (0.952 + Pr)^{-1/4} (Ra_x)^{1/4}$	Eckert and Drake [15]
Electronic cooling	Nu = a (Ra*) ^b , where a = 0.906{1+0.011/(W/W _∞) ^{3.3965} } ^{0.2745} b = 0.184{1+2.64 x 10 ⁵ /(W/W _∞) ^{9.248} } ^{-0.0362}	Park and Bergles [27]
	$Nu_{L/2} = [12/Ra + 1.8/(Ra)^{0.4}]^{-0.5}$	Bar-Cohen and Schweitzer [29]

Continued

Table-B: Review Works on Different Type of Fin Profile.

Fin Profile Type	Correlations	Author
Arbitrary shape	$Nu_L = \frac{Nu_{\sqrt{A_s}} \cdot L}{\sqrt{A_s}} \text{ or } Nu_L = \frac{Nu_{\sqrt{A_s}} \cdot b}{\sqrt{A_s}}$	Hassani and Hollands [21]
Vertical rectangular fin arrays	$Nu_L = 0.112 \left(Ra_L \cdot \frac{b}{L} \right)^{0.534} \left[1 - e^{-129 / \left(Ra_L \cdot \frac{b}{L} \right)} \right]^{0.284}$	J.B. Chaddock [20]
Triangular fin arrays	$Nu_L = \frac{Q_{conv} \cdot L}{A_s \Delta T K}; \text{ where, } Q_{conv} = VI - \sigma A_s \epsilon [\bar{T}_b^4 - T_a^4]$	Karagiozis, Raithby and Hollands [13]

Table-C: Heat Transfer Enhancement due to Increase of Ra for Different Fin Arrays.

Sl. No.	Single Fin with Flat Plate			Array of 4 Fins			Array of 7 Fins			Array of 13 Fins		
	Q_{fin}	$Q_{eqv.unfin}$	Q_{Tot}	Q_{fin}	$Q_{eqv.unfin}$	Q_{Tot}	Q_{fin}	$Q_{eqv.unfin}$	Q_{Tot}	Q_{fin}	$Q_{eqv.unfin}$	Q_{Tot}
1	.0051	.005	.0390	.0430	.030	.1790	.205	.090	.7000	.183	.100	.0930
2	.0110	.010	.5790	.1198	.068	.3788	.405	.151	1.1440	.427	.120	1.2120
3	.0200	.018	.9210	.1740	.090	.6970	.632	.214	1.8120	1.070	.300	3.0100
4	.2520	.225	.9314	.5560	.248	1.6950	1.330	.420	3.2100	2.770	.830	7.1480
5	-	-	-	1.247	.502	2.4630	6.670	2.030	14.079	20.38	6.00	40.370

Graph of Table-C is shown in Fig. 17a

APPENDIX-C: MATHEMATICAL EQUATIONS OF REVIEW WORKS

C.1 Equations of Different Profiles for Efficiency and Optimum Shape

To show the reasons of selection of triangular fin arrays; efficiency and optimum profile of different fin profiles are discussed below:

From P. J. Schneider [26] the followings are mentioned.

- a. Fin of rectangular profile:

$$e^a = \frac{1}{\sqrt{2\xi}} \tanh \sqrt{2\xi}$$

$$\xi = H_c^{M2} \sqrt{h / kA}$$

$$[A = H \cdot t]$$

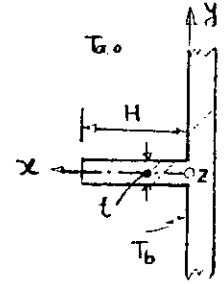


Fig.1: Rectangular fin.

- b. Straight trapezoidal fin profile:

$$e^b = \frac{\pi k \eta_2 \tan \theta}{4hH} \left[\frac{I_1(\eta_2)k_1(\eta_1) - I_1(\eta_1)k_1(\eta_2)}{I_0(\eta_2)k_1(\eta_1) - I_1(\eta_1)k_0(\eta_2)} \right]$$

where,

$$\eta^2 = 4c^2 [x + \delta_1(1 - 2 \tan \theta) / 2 \tan \theta]$$

$$\text{and } c = (h/k \sin \theta)^{1/2}$$

Now, considering $\eta_1 = \eta_{x=0} = 0$, $\eta_2 = \eta_{x=H} = 2c\sqrt{H}$

$$e^b = \left(\frac{1}{\xi} \right) \frac{I_1(2\xi)}{I_0(2\xi)} \quad [\because \sin \theta = \theta = \tan \theta \text{ for } \theta = 0]$$

$$\text{or } e^b = e^c$$

- c. Fin of triangular profile:

$$e^c = \left(\frac{1}{\xi} \right) \frac{I_1(2\xi)}{I_0(2\xi)}$$

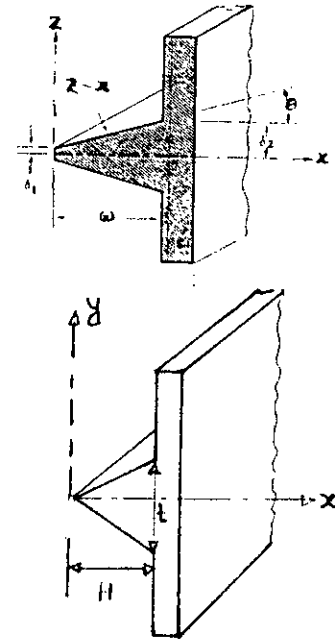


Fig.2: Triangular and trapezoidal fin.

d. Fin of parabolic profile (inward):

$$e^d = \frac{2}{1 + \sqrt{1 + \frac{8}{3} \xi^2}}$$

e. Fin of parabolic profile (outward):

$$e^e = \frac{1}{\sqrt{\frac{4}{3} \xi}} \frac{I_{2/3}[(4/3)^{3/2} \xi]}{I_{-1/3}[(4/3)^{3/2} \xi]}$$

From above equations $e^c > e^d \gg e^e > e^b > e^a$.

e vs. ξ curve is shown in Fig. 4

Again considering optimum profiles:

$$A^a = \frac{0.252}{h^2 k} \left(\frac{q_0}{T_{b'}} \right)^3$$

$$A^c = \frac{0.174}{h^2 k} \left(\frac{q_0}{T_{b'}} \right)^3$$

$$A^d = \frac{0.167}{h^2 k} \left(\frac{q_0}{T_{b'}} \right)^3$$

[q_0 = heat transfer at $x = 0$ for rectangular fin
 $x = H$ for others]

where, "a" denotes rectangular fin, "c" denotes straight triangular fin and "d" denotes fin of inward parabolic profile.

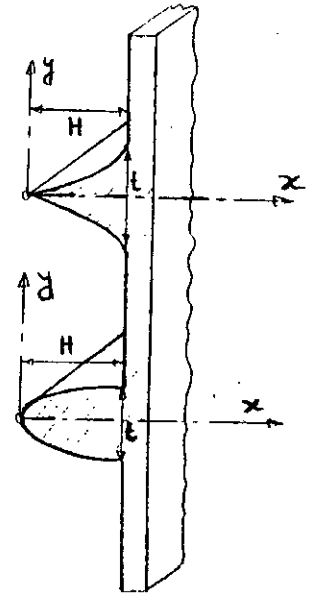


Fig.3: Parabolic fin.

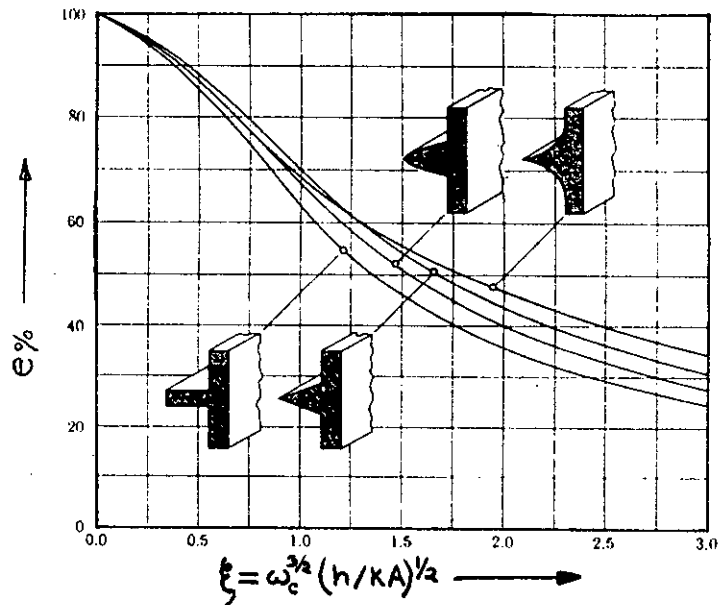


Fig.4: Efficiency vs. emissivity (ϵ) curve.

Inward parabolic fin having the least profile area and rectangular fin, triangular fin need 51% and 4% more material respectively than least profile. **Considering all aspects, we have selected the triangular fin profile in the array for further study.** Indeed straight triangular fins performance approaches quite closely that of the optimal shape (Eckert & Drake, 1972) [1].

C.2 Prominent Scientists' Works Of Different Profiles

C.2a Heat Transfer From Vertical Flat Plate

Hellums and Churchill [14] applied the technique of dimensional analysis to natural convection as follows:

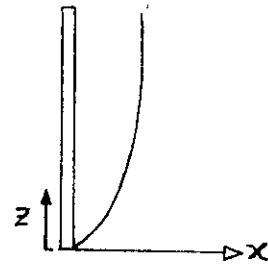


Fig.5: Vertical flat plate.

Case	Assumptions	Relationships
A	1, 2, 3, 4, 5, 6	$\frac{h}{k} \left(\frac{\alpha \nu L}{g \beta \Delta T} \right)^{1/4} = f \left(\frac{\nu}{\alpha} \right)$

[Assumptions: 1 = Infinite vertical plate, 2 = Newtonian Fluid, 3 = Constant transport properties, 4 = Negligible viscous dissipation and work of compression, 5 = $\beta \Delta T \ll 1$, 6 = thin boundary layer assumptions.]

Case A, can be rewritten as:

$$Nu_x = f(Pr) \cdot (Ra_x)^{1/4} \quad (5)$$

A form of equation (5) developed for the vertical plate from integral boundary layer analysis by Eckert and Drake [15], is

$$Nu_x = 0.508 Pr^{1/4} (0.952 + Pr)^{-1/4} (Ra_x)^{1/4}$$

Considering $Pr = 0.71$ for air, the above equation becomes

$$Nu_L = 0.515 (Ra_L)^{1/4} \quad (6)$$

Comparison of the above equation with experimental data is shown in Fig. 17b.

C.2b Natural Convection Heat Transfer From Vertical Parallel Plates

This type of problem is more complex than single vertical flat plate due to “Core” region as well as the boundary layer. As noted by Ostrach [16], “the boundary layer and the core are closely coupled to each other, and this coupling constitutes the main source of difficulty is obtaining analysis solutions to internal problems”.

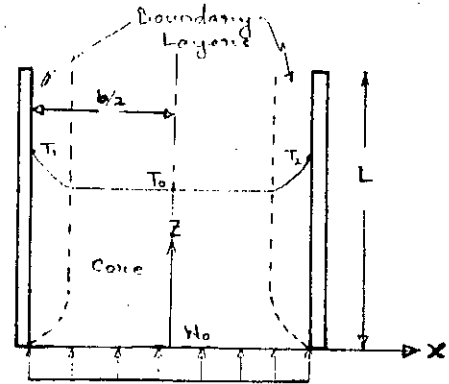


Fig.6: Vertical parallel plates.

Bodoia and Osterle [17] made a numerical solution for vertical parallel plates. Their results using dimensionless length, $2L/(b.Gr)$ for narrow channel was

$$Nu_L = \frac{1}{24} \frac{b}{L} (Gr, Pr) = \frac{1}{24} \frac{b}{L} (Ra_L) \quad (7)$$

For wide plate separation: $Nu_L = 0.680 (Ra_L b / L)^{1/4}$ (8)

Originally Elenbaas [18, 19] made a semi-empirical equation for free convection of parallel plates.

$$Nu_L = \frac{1}{24} \frac{b}{L} Ra_L \left[1 - e^{-35 / \left(\frac{b}{L} \right) Ra_L} \right]^{3/4} \quad (9)$$

Elenbaas showed the optimum spacing of isothermal parallel vertical plates:

$$Gr_o \cdot Pr \left(\frac{B_o}{L} \right) \cong 50 \quad (10)$$

Where $B_o =$ optimum plate/fin spacing
 $Gr_o = \frac{g\beta\Delta T B_o^4}{Lv^2}$

C.2c Natural Convection Heat Transfer From Vertical Rectangular Fin Arrays

Elenbaas type equation was used by J. B. Chaddock [20] for rectangular fin arrays,

$$Nu_L = 0.112 \left(Ra_L \frac{b}{L} \right)^{0.534} \left[1 - e^{-129 / \left(Ra_L \frac{b}{L} \right)} \right]^{0.284} \quad (11)$$

Here, as in the case of the circular fin-on-tube results of Edward's and Chaddock [20], the correlation curve has the characteristics slope of 0.25 at high Rayleigh numbers. The slope of 0.534 at the low end of the curve is also in close agreement with the fin-on-tube results. The equation (11) has also close agreement with that of Elenbaas' equation for vertical plates at high Rayleigh number. The comparison of our experimental data with equation (11) is shown in Fig. 20.

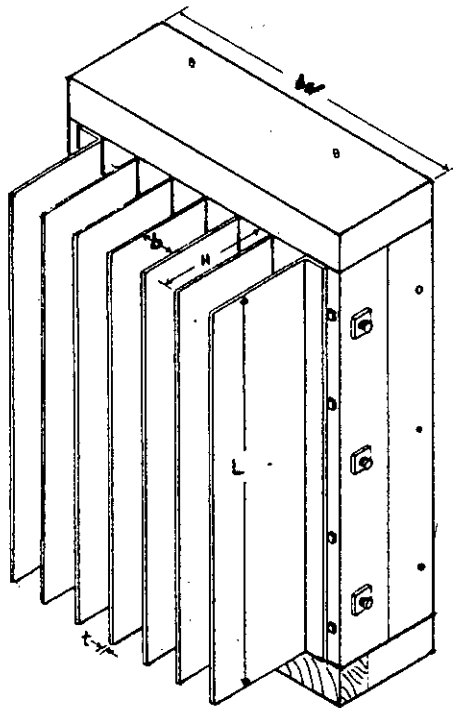


Fig.7: Rectangular fin arrays.

C.2d Natural Convection Heat Transfer From Triangular Fin Arrays

A. Karagiozis, G. D. Raithby and K. G. T. Hollands [13] have made the empirical solution for triangular fin arrays using the conception of rectangular fins that is "the triangular fin will convect the same as rectangular fin of the same perimeter facing a passage of the same cross-sectional area".

$$Nu_1 = \frac{Q_{conv} L}{As \Delta T k} \quad (12a)$$

$$Q_{Tot} = VI = Q_{conv} + Q_{Rad} + Q_l$$

$$\Rightarrow VI = Q_{conv} + \sigma A_s F_{1-2} (\bar{T}_{b'}^4 - T_a^4) + Q_l$$

$$\Rightarrow VI = Q_{conv} + \sigma A_s F_{1-2} (\bar{T}_{b'}^4 - T_a^4) \quad (12b)$$

$$\Rightarrow Q_{conv} = VI - \sigma A_s F_{1-2} (\bar{T}_{b'}^4 - T_a^4)$$

[∴ $Q_l = \text{negligible}$]

where F_{1-2} is the radiant exchange factor.

Combining equation 12(a) and 12(b) Raithby and Hollands solved the problem by transient method. Their conclusions were: (a) Nusselt number for the vertical orientation is upto 87 percent higher than for the horizontal orientation (b) for $Ra < 4000$, Nu value depends on N_{cond} only, which will change with geometry, (c) $Ra \geq 4000$ triangular fin arrays behave like a flat plate. The outcome of their experiment is shown in Fig. 20 and our experimental data also plotted in the same Figure.

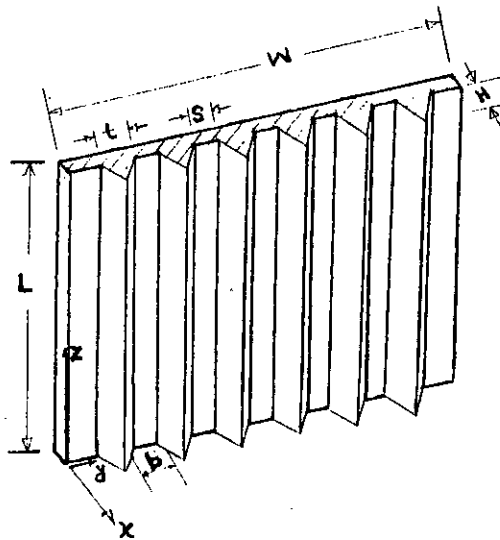


Fig.8: Triangular fin arrays.

C.2e Natural Convection Heat Transfer From Arbitrary Shape

A. V. Hassani and K. G. T. Hollands [21] have introduced an equation for an arbitrary shape for free heat convection. The equation is

$$Nu_{\sqrt{A_s}} = \left[\left[(\bar{C}_t Ra_N^{1/4})^m + (\hat{C}_t Ra_N^{1/3})^m \right]^{n/m} + (Nu_{c, \sqrt{A_s}})^n \right]^{1/n} \quad (13a)$$

$$\text{or } Nu_{x=L} = \frac{Nu_{\sqrt{A_s}} \cdot L}{\sqrt{A_s}} \text{ or } Nu_{x=b} = \frac{Nu_{\sqrt{A_s}} \cdot b}{\sqrt{A_s}} \quad (13b)$$

[Where,

$$\bar{C}_t = 0.671 [1 + (0.492 / Pr)^{9/16}]^{-4/9}$$

$$N = (L \cdot \bar{P}^2)^{1/3}$$

$$Ra_N = \frac{g \beta \Delta T N^3}{\nu \alpha}$$

\bar{P} = perimeter averaged over the total height of the body, m

$$= \frac{1}{L} \int_0^L f_o^x f_o^y h_y dy \cdot dL$$

(h_y = length scale on the surface of a body in the direction orthogonal to the streamline)

$$m = 2.5 + 12.0 e^{-13[\hat{C}_t Ra_N^{1/12} - 0.5]}$$

$$\hat{C}_t = \bar{C}_t \sqrt{A_s} / N$$

$$\bar{C}_t = 0.098 - (0.065) \frac{A_h}{A_s} + 0.008 \frac{L \bar{P}}{A_s}$$

A_h = horizontal downward facing surface of a heated body or horizontal upward facing surface of a cooled body, m²

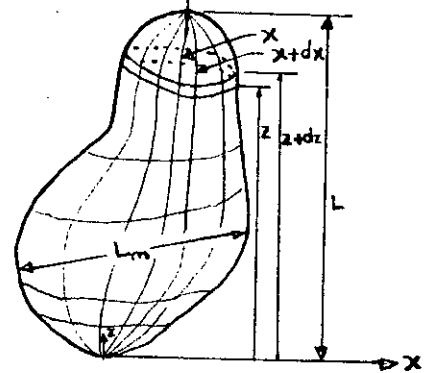


Fig.9: Arbitrary shape.

$$n = \left[1.26 - \frac{(2 - \sqrt{A_s / L_m})}{9\sqrt{1.0 - 4.79 v^{2/3} / A_s}}, 1.0 \right]_{\max}$$

= 1.07 (average value)

v = Volume of the body, m^3

L_m = longest straight line passing through the body, m

$Nu_{c, \sqrt{A_s}}$ = conduction Nusselt of the body = 3.51

If $Ra_N < \left(\frac{\bar{C}_l}{\hat{C}_l} \right)^{12}$, then right hand side 2nd term of equation (9a) can be neglected.]

Equation (13b) is applicable to an any irregular shape. In the present experiment triangular fin arrays can be considered as irregular or arbitrary shape as the fins are integrated part of the base plate (Fig. 21). Comparison of experimental data and equation (13b) is shown in Fig. 13 to Fig. 16.

C.2f Natural Convection Heat Transfer from Electrical & Electronic Equipment

Park and Bergles [27] extended Baker's [28] early work to determine heat transfer coefficients for small single heaters flush-mounted on vertical surfaces and immersed in R-113. The results were correlated in the form of equation 14a below.

$$Nu = a(Ra^*)^b \quad [14a]$$

where

Ra^* = flux-based Rayleigh number

$$a = 0.906 \{ 1 + 0.011 / (W/W_\infty)^{3.3965} \}^{0.2745}$$

$$b = 0.184 \{ 1 + 2.64 \times 10^5 / (W/W_\infty)^{9.248} \}^{-0.0362}$$

W is the width of the heater and W_∞ is 70 mm

and

$$2 \times 10^5 < Ra^* < 2 < 10^8$$

$$0.03 < W/W_\infty < 1$$

The Bar-Cohen and Schweitzer [29] relation for the symmetrically-heated isoflux channel Nusselt number, based on the mid-height temperature is shown in equation 14b and is typical of their results.

$$\text{Nu}_{L/2} = [12/\text{Ra} + 1.8/(\text{Ra})^{0.4}]^{-0.5} \quad [14b]$$

Using relations such as these, it is possible to obtain the mid-height, as well as maximum, surface temperature for a densely-packaged board under all operating conditions. It is, furthermore, possible to specify the plate spacing for which the total heat transfer rate is maximized or, alternately, the board spacing required to achieve the lowest possible surface temperature. For the likely range of convective heat fluxes and board dimensions, board spacings of less than 5 mm were found to maximize the volumetric cooling capability of such configurations.

C.2g Surrounding Effect Of A Heated Body

According to A. Karagiozis, G. D. Raithby and K. G. T. Hollands [13] the outer surface, far removed from the heating body, can be assumed to be a sphere, of radius R_o , centered at the origin.

Therefore,

$$\begin{aligned} \sqrt{x^{*2} + y^{*2} + z^{*2}} &= R_o^* = \frac{R_o}{b}; \\ u^* = v^* = w^* = \theta &= \frac{T_a - T_a}{T_{b'} - T_{b'}} = 0 \end{aligned} \quad (15)$$

If R_o^* is not large, there will be hydrodynamic and thermal interference between the fin array and the outer surface (i.e., enclosure effects).

APPENDIX-D: UNCERTAINTY

The term “uncertainty” is used to refer to “a possible value that an error may have”. Kline and McClintock (1953) [25] attributed this definition and it still seems an appropriate and valuable concept.

Now suppose, a set of measurement is made and the uncertainty in each measurement may be expressed with the same odds. These measurements are then used to calculate some desired result “R” using the independent variables $x_1, x_2, x_3, \dots, x_n$;

where,

$$R = R(x_1, x_2, x_3, \dots, x_n) \quad 16(a)$$

Let, $W_1, W_2, W_3, \dots, W_n$ be the uncertainties in the independent variables given with the same odds. Then the uncertainty W_R in the result having these odds is given in Kline and McClintock [1953] as,

$$W_R = \left[\left(\frac{\partial R}{\partial x_1} W_1 \right)^2 + \left(\frac{\partial R}{\partial x_2} W_2 \right)^2 + \dots + \left(\frac{\partial R}{\partial x_n} W_n \right)^2 \right]^{\frac{1}{2}} \quad 16(b)$$

where, the partial derivative of R with respect to x_i is the sensitivity coefficient for the result R with respect to the measurement x_i .

If, $R = x_1^a, x_2^b, x_3^c, \dots, x_m^n$

Then,

$$\frac{W_R}{R} = \left[\left(a \frac{w_1}{x_1} \right)^2 + \left(b \frac{w_2}{x_2} \right)^2 + \dots + \left(m \frac{w_m}{x_m} \right)^2 \right]^{\frac{1}{2}}$$

In the present experiment errors in different calculations are as follows:

Temperature = $\pm 0.95\% = 0.0095$

Emissivity = $0.2\% = 0.002$

Resistance of heater = $2.4\% = 0.024$

Current = $0.1\% = 0.001$

Uncertainty in Convective Heat Transfer, Q_{conv} :

$$\begin{aligned} Q_{conv} &= I^2 R - A_s \sigma \epsilon (\bar{T}_b^4 - \bar{T}_a^4) \\ &\cong I^2 R - \epsilon T^4 \left[\begin{array}{l} I = .38 \pm .001; R = 111.14 \pm .024; \\ \epsilon = .63 \pm .002; T = 43.8571 \pm .0095 \end{array} \right] \\ \therefore \frac{W}{Q_{conv}} &= \left[\left(2 \frac{W_I}{I} \right)^2 + \left(\frac{W_R}{R} \right)^2 \right]^{\frac{1}{2}} - \left[\left(\frac{W_\epsilon}{\epsilon} \right)^2 + \left(4 \frac{W_T}{T} \right)^2 \right]^{\frac{1}{2}} \\ &= \left[\left(2 \frac{.001}{.38} \right)^2 + \left(\frac{.024}{111.14} \right)^2 \right]^{\frac{1}{2}} - \left[\left(\frac{.002}{.63} \right)^2 + \left(4 \frac{.0095}{43.8571} \right)^2 \right]^{\frac{1}{2}} \\ &= .005267 - .00325 = \pm 0.19\% \end{aligned}$$

Uncertainty in Nusselt Number, Nu :

From Table-4, Sl. No. 7, $Q_{conv} = 7.634 \pm .0019$
 $\Delta T = 13.2571 \pm .0095$

$$Nu = \frac{Q_{conv} B}{A_s K_F \Delta T} \cong Q_{conv} \Delta T^{-1}$$

$$\begin{aligned} \therefore \frac{W}{Nu} &= \left[\left(\frac{W_{Q_{conv}}}{Q_{conv}} \right)^2 + \left(-1 \times \frac{W_{\Delta T}}{\Delta T} \right)^2 \right]^{\frac{1}{2}} \\ &= \left[\left(\frac{.0019}{7.634} \right)^2 + \left(-1 \times \frac{.0095}{13.2571} \right)^2 \right]^{\frac{1}{2}} = \pm 0.075\% \end{aligned}$$

Uncertainty in Rayleigh Number, Ra :

Here,

$$Ra = \frac{g \beta B^4 \Delta T}{\nu \alpha L} \cong \Delta T; \Delta T = 13.2571 \pm .0095$$

$$\therefore \frac{W}{Ra} = \left[\left(\frac{.0095}{13.2571} \right)^2 \right]^{\frac{1}{2}} = 0.072\%$$

APPENDIX-E

SPECIFICATIONS OF NON-CONTACT INFRARED THERMOMETER

Model No	:	IT - 330
Range	:	0 to 300°C (Display : -50 to 300°C)/-58° to 572°F
Resolution	:	0.1°C (in range -50.0 to 199.9°C) 1°C (range 200 to 300°C)
Accuracy	:	± 1% ± 1 digit of full scale (at emissivity $\epsilon = 1$, ambient temperature 20 to 30°C)
Emissivity Setting:	:	0.10 to 1.00 (in 0.01 increments)
Response	:	Approximate 2 sec.
Readout	:	Emissivity and set, maximum, average and minimum temperatures (selected by MODE Key)
Alarm	:	over range (below -50°C or above 300°C), battery life.
Power supply	:	4 x AAA batteries
Measurement Wavelength Range	:	6 to 12 μ m
Operating Temperature	:	0 to 50°C at 85% RH or less
Storage Temperature	:	20 to 50°C at normal humidity
Dimensions Body	:	140 (W) x 60 (D) x 27 (H) mm/5.5 (W) x 2.4(D) x 1.1 (W) in
Probe	:	140 (L) x 25 (W) mm (excluding protrusions) /5.5 (L) x 0.98 (W) in

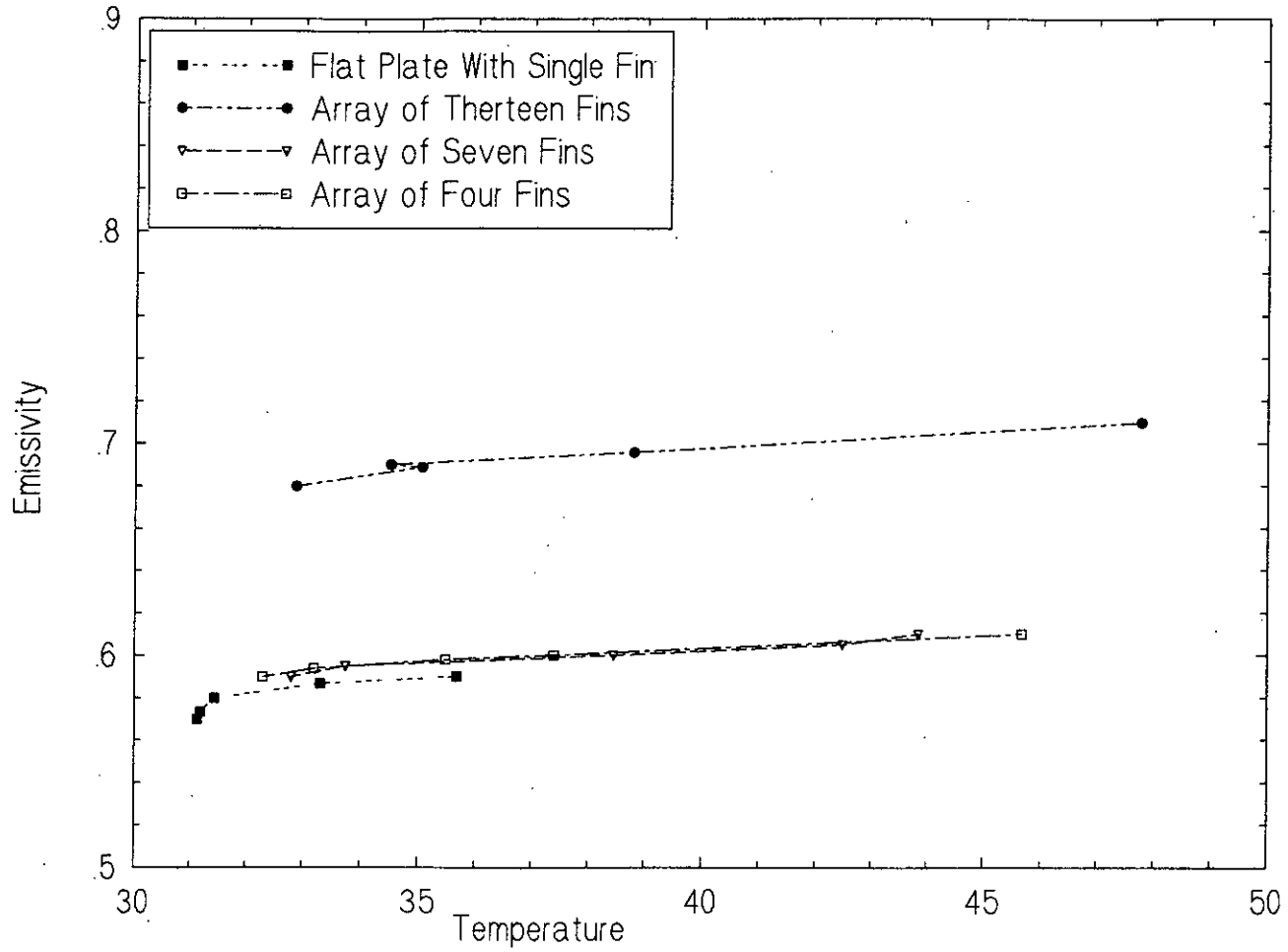


Fig.10 :Effect of temperature on emissivity for different fin arrays.

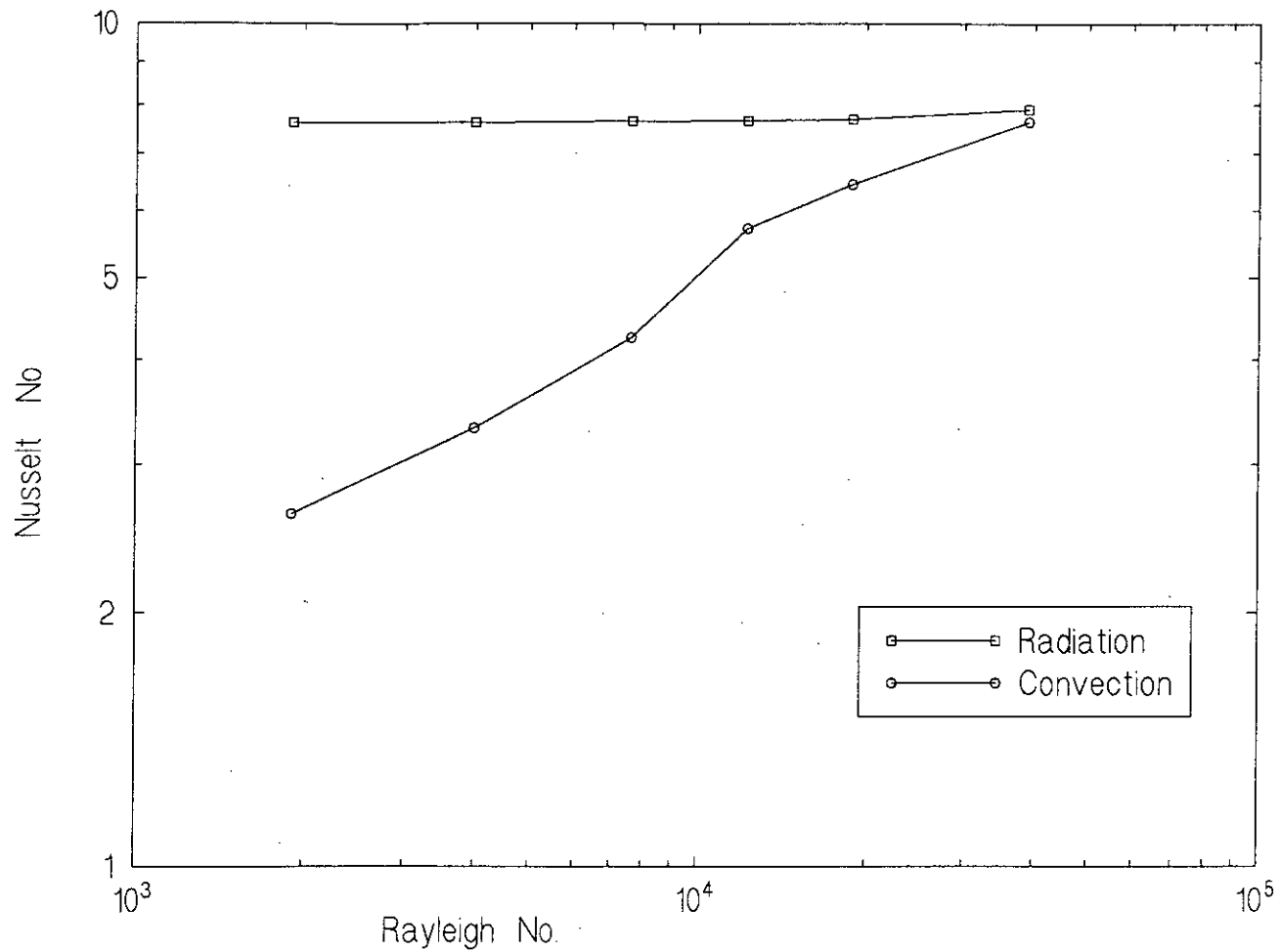


Fig.11a:Effect of radiation heat loss on conv.heat loss from an array of 4 fins

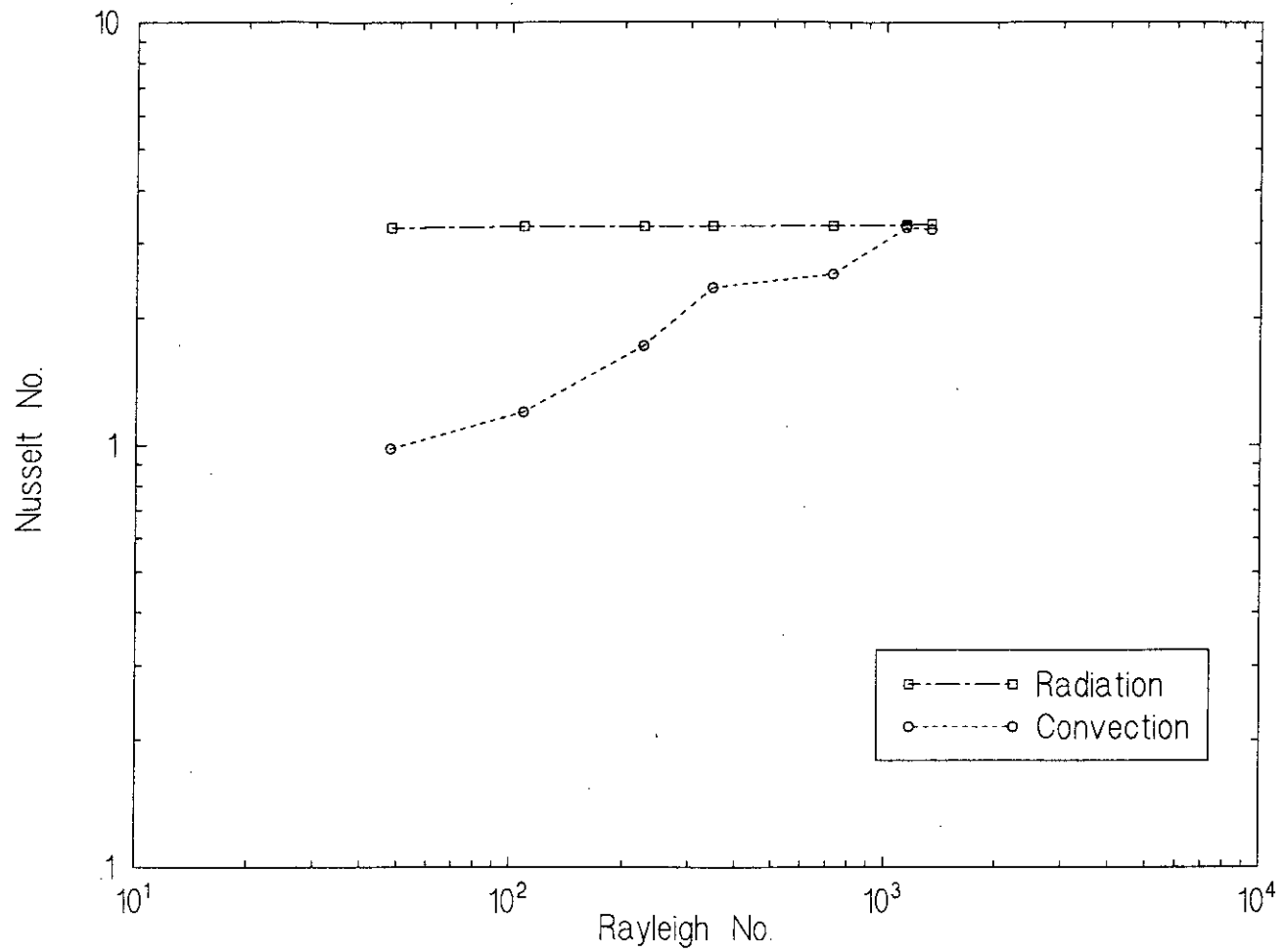


Fig.11b:Effect of radiation heat loss on conv.heat loss from an array of 7 fins

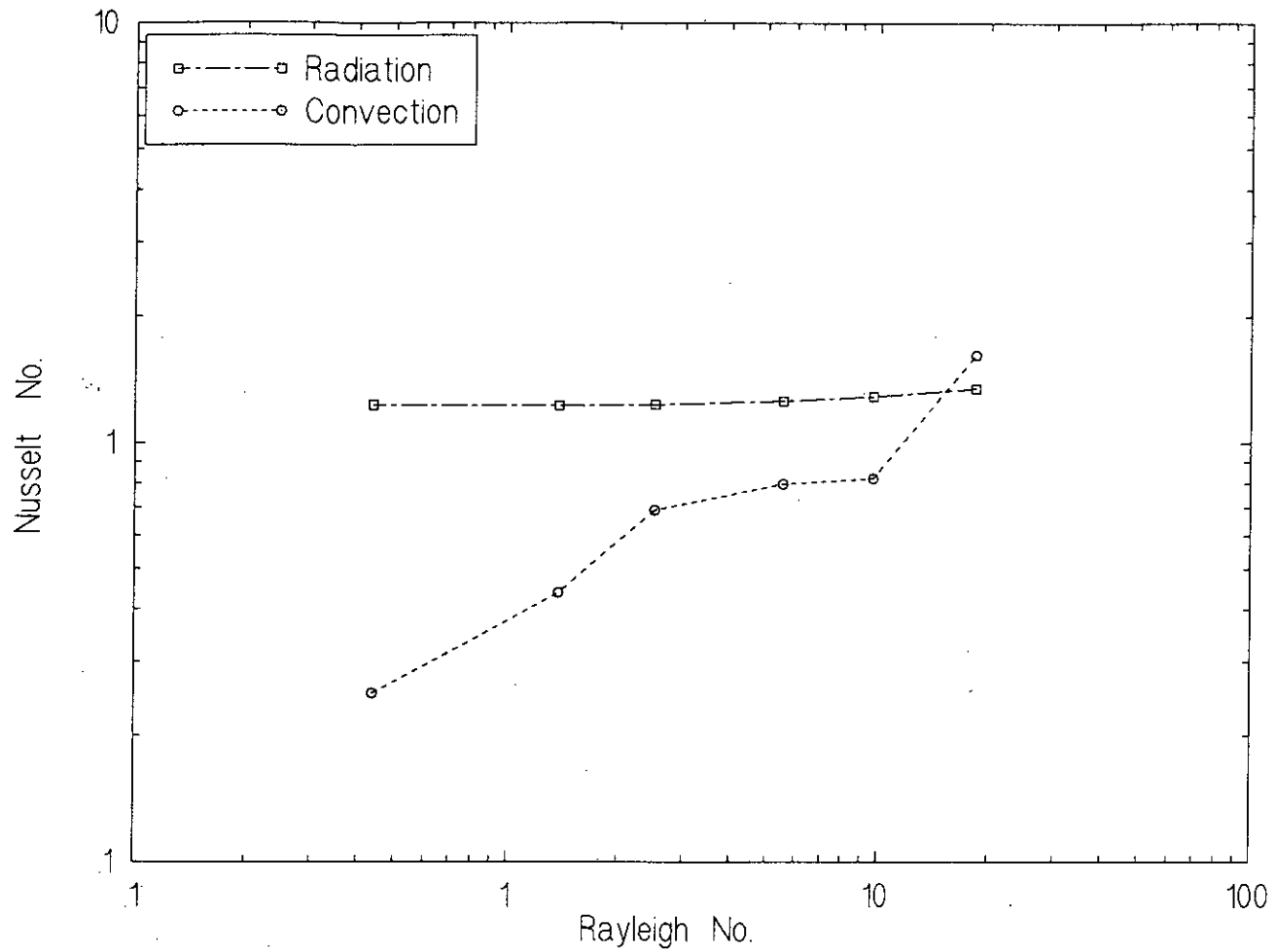


Fig.11c.Effect of radiation heat loss on conv.heat loss from an array of 13 fins

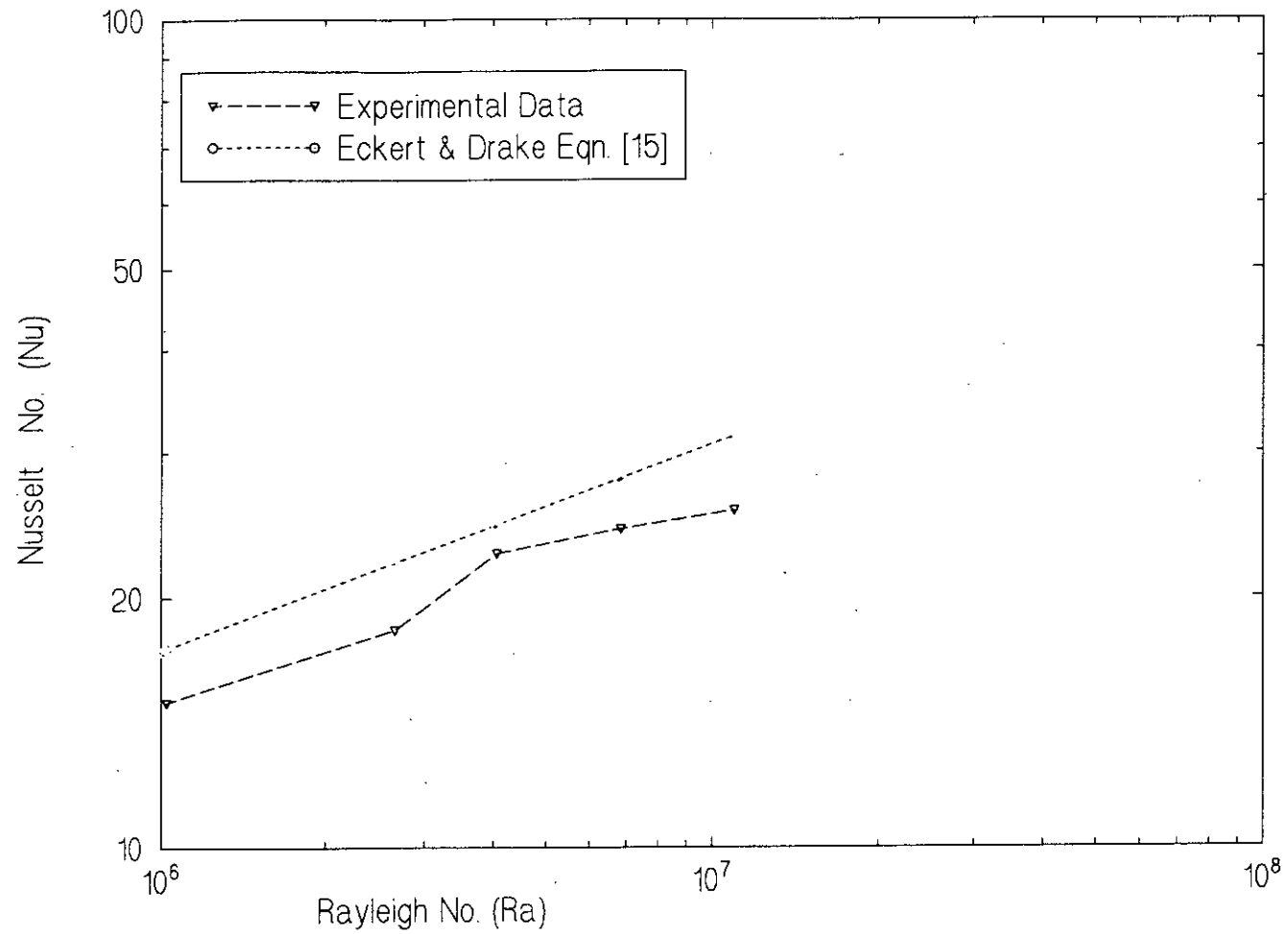


Fig.12: Log-log plot of observed Nu no VS Ra no for vertical flat plate

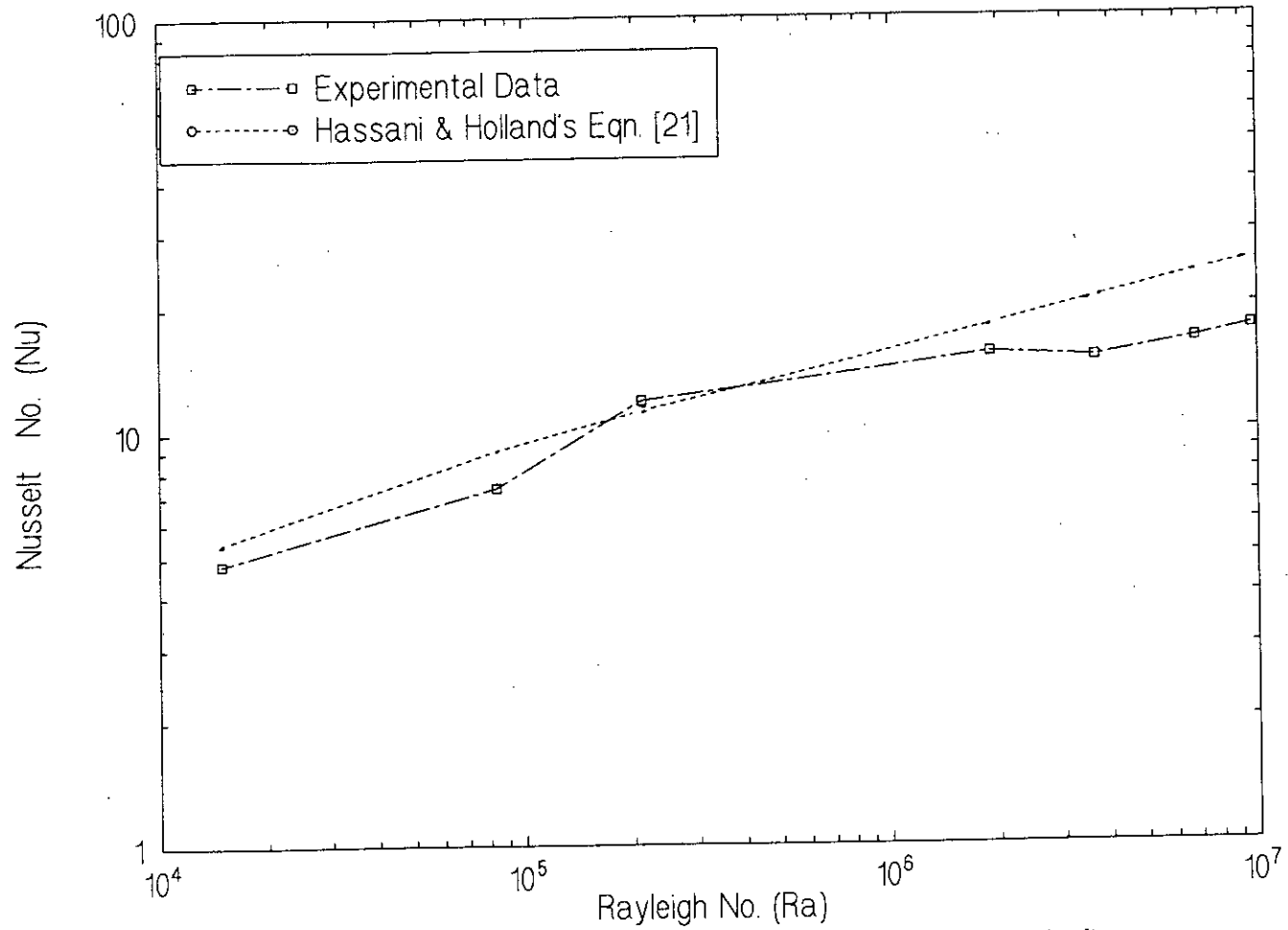


Fig.13 : Log-log plot of observed Nu no Vs Ra no for single fin

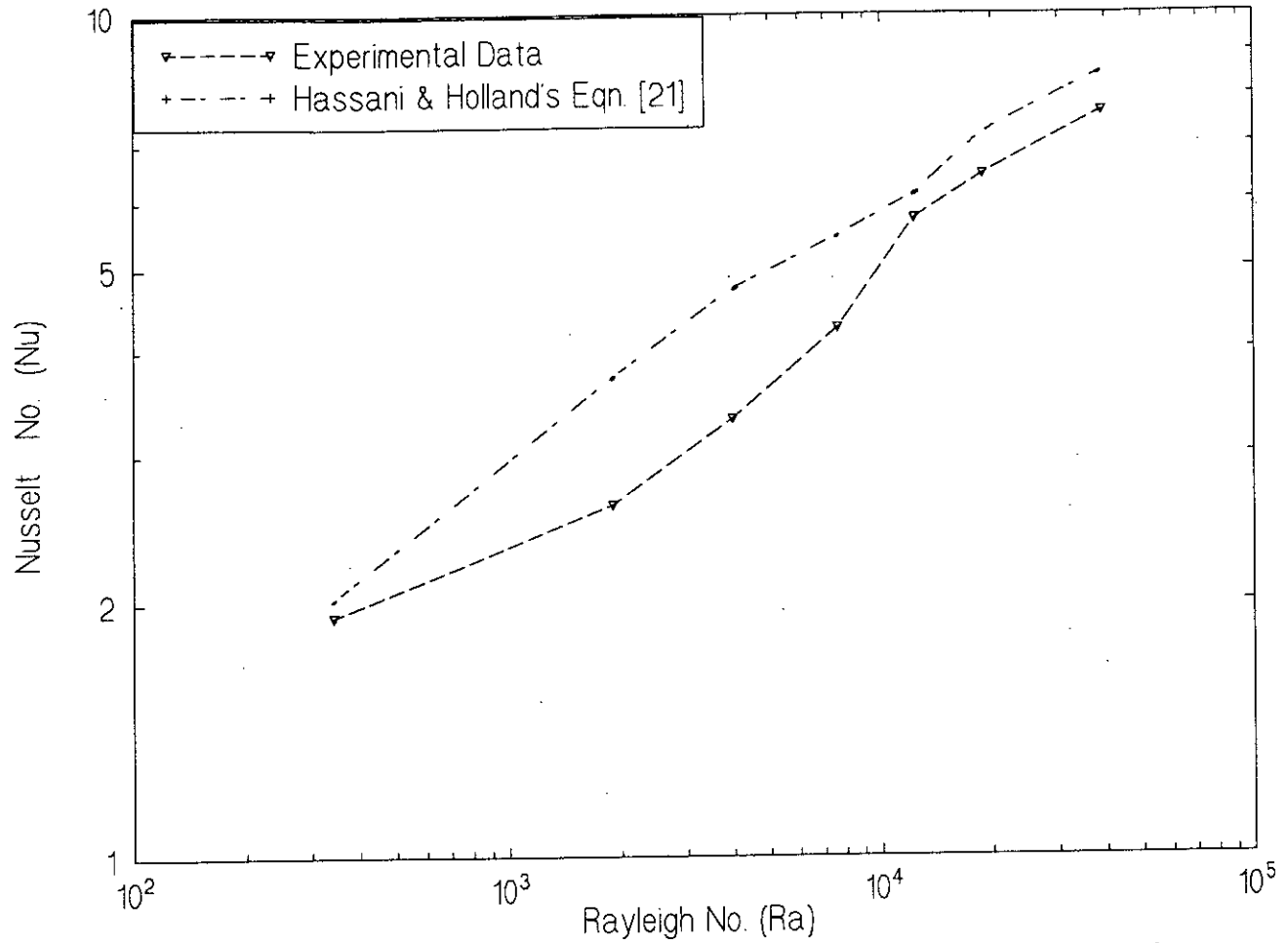


Fig14 :Log-log plot of observed Nu no Vs Ra no for an array of four fins.

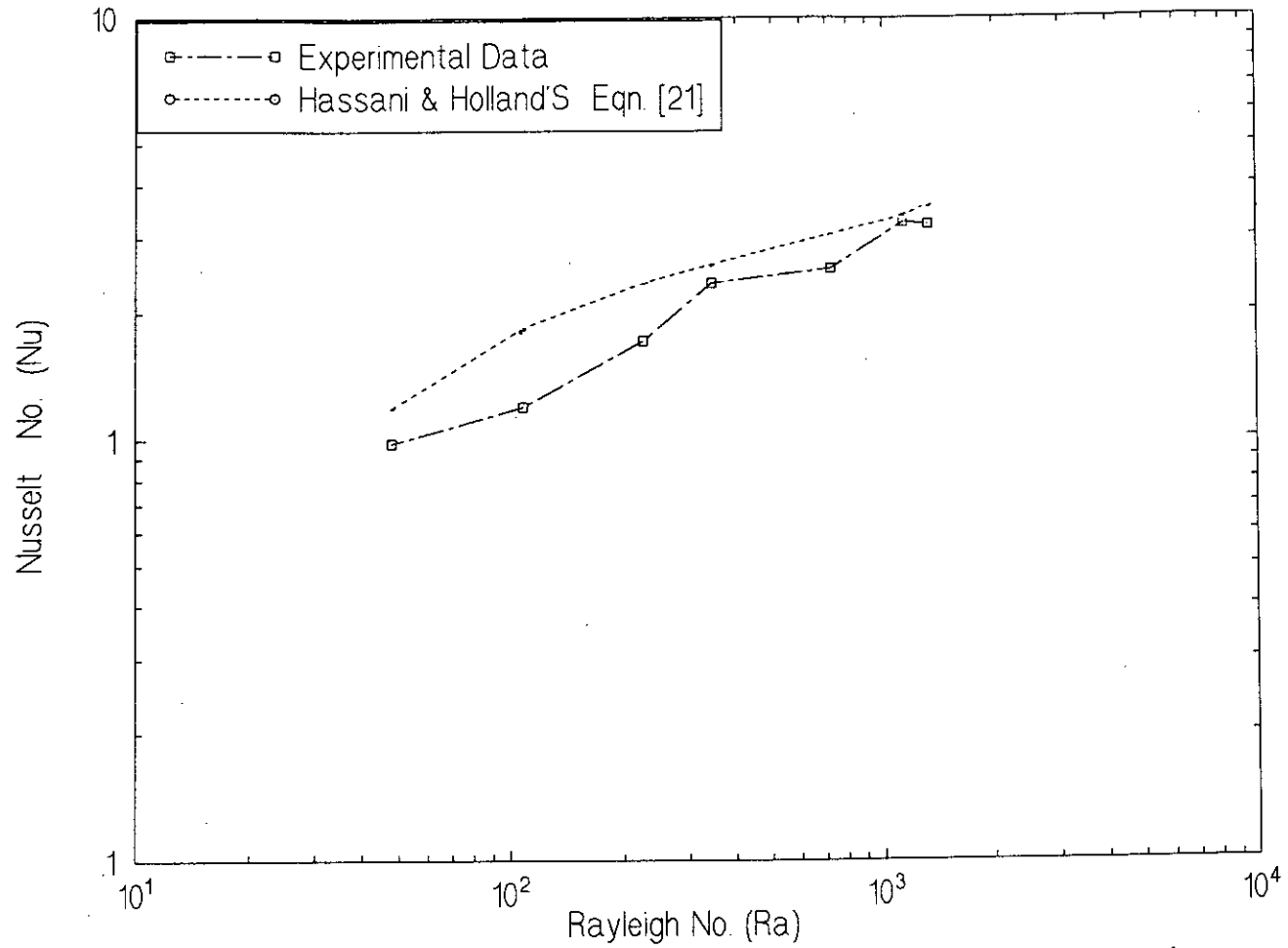


Fig.15 : Log-log plot of observed Nu no Vs Ra no for an array of seven fins.

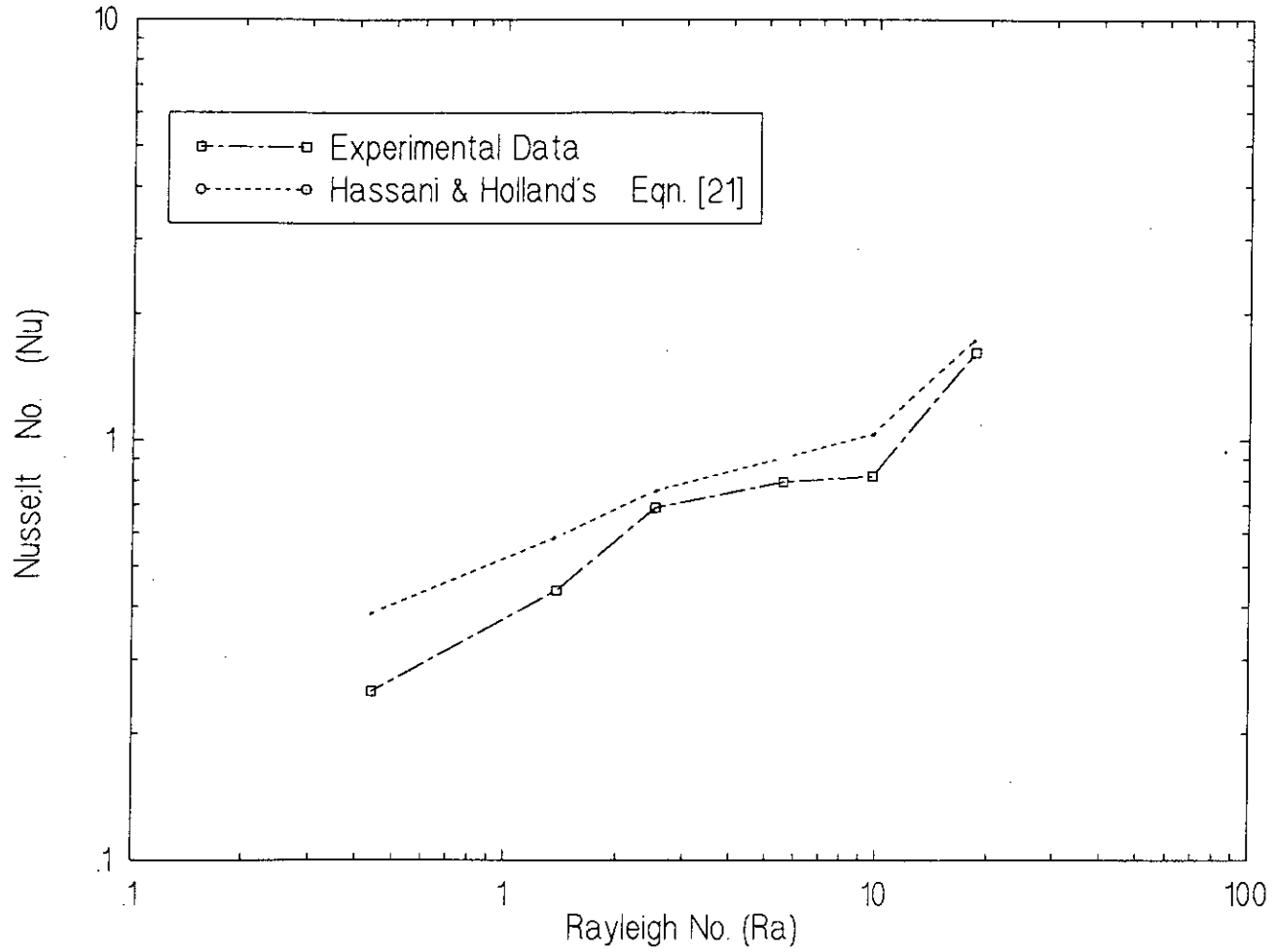
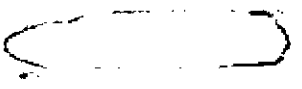


Fig.16 : Log-log plot of observed Nu no Vs Ra no for an array of thirteen fins



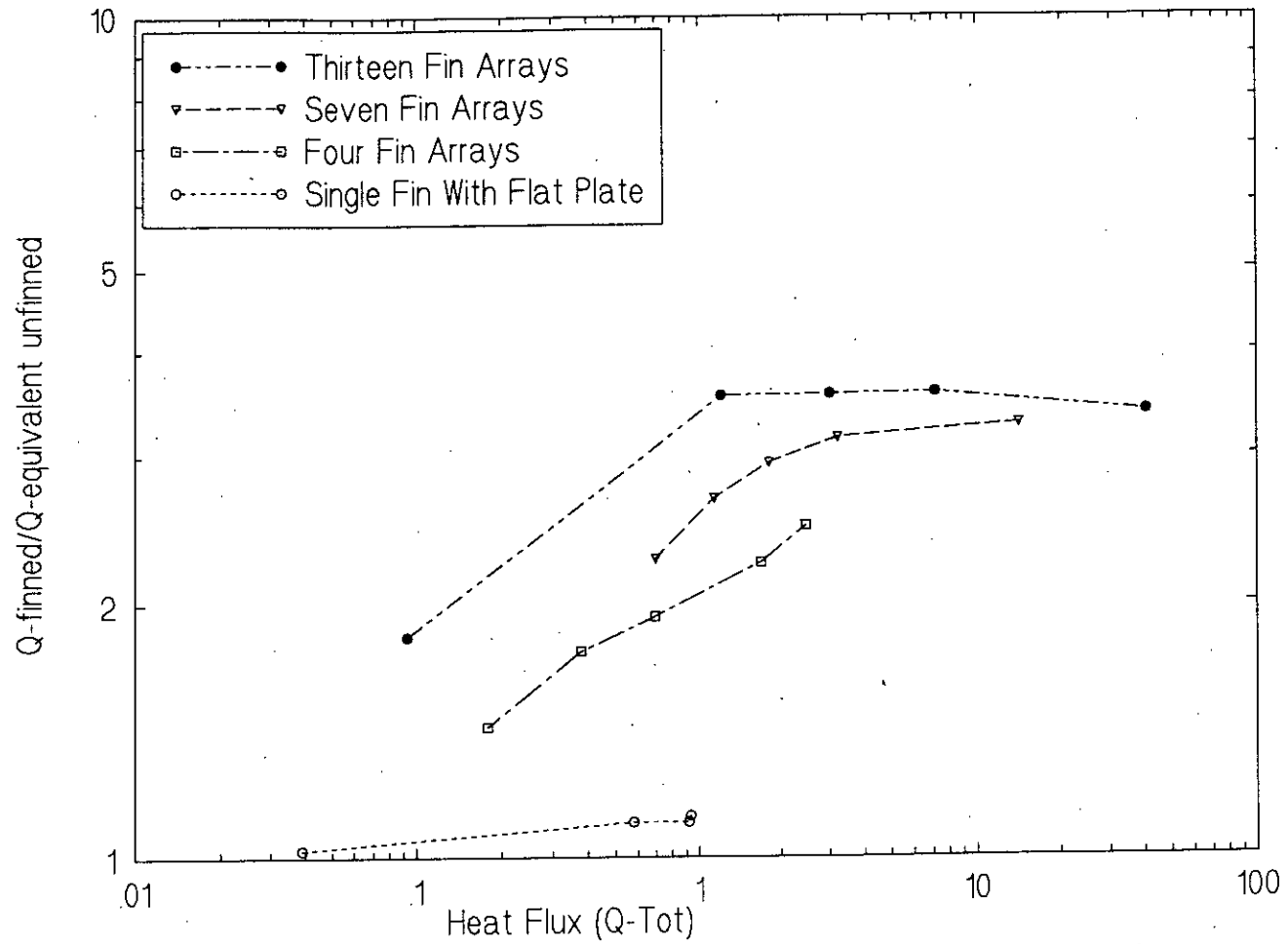


Fig.17a: Heat transfer enhancement due to increase of Ra for different fin arrays.

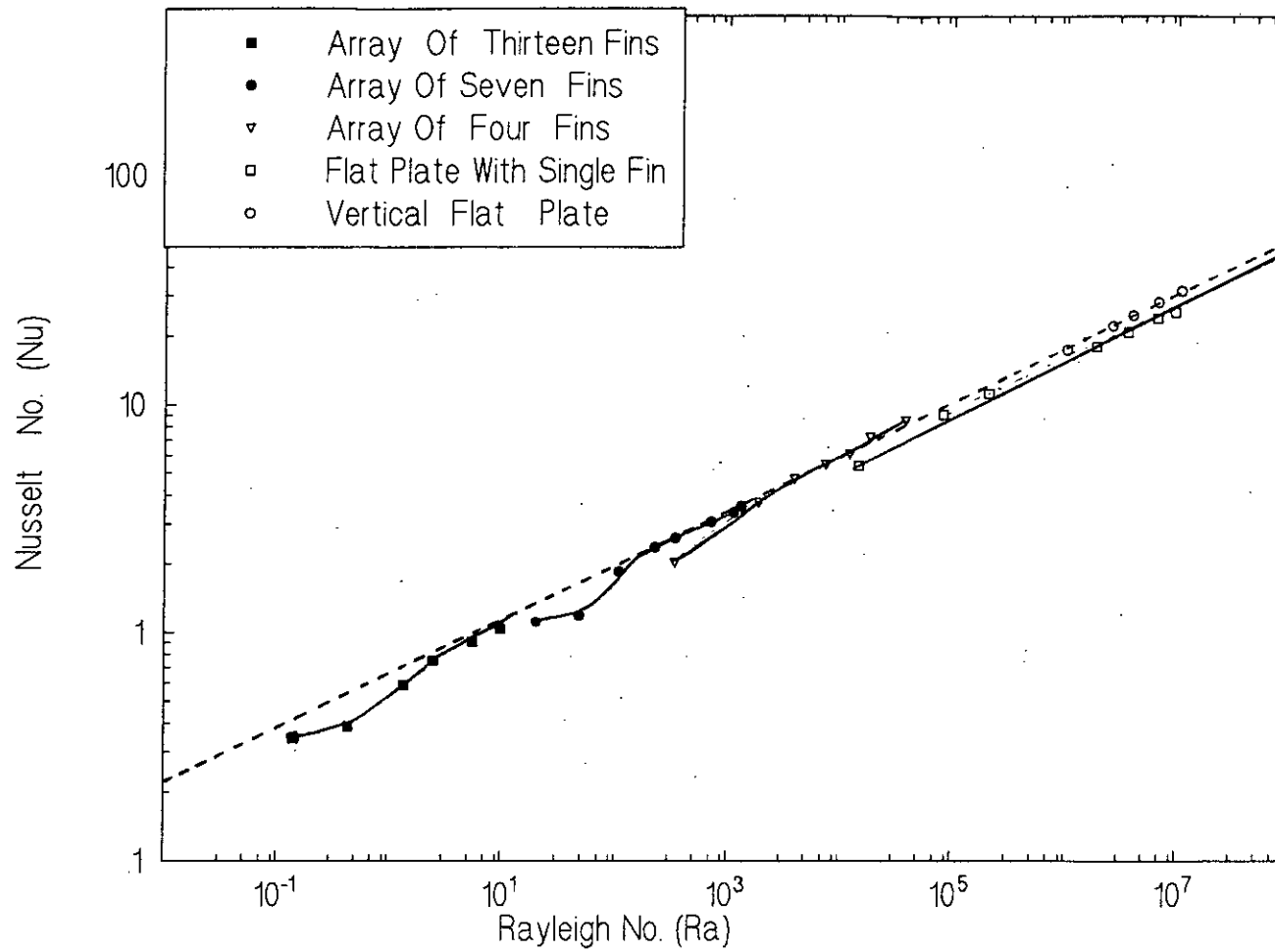


Fig.17b: Log-log plot of observed Nu No Vs Ra No for difeerent fin concentration

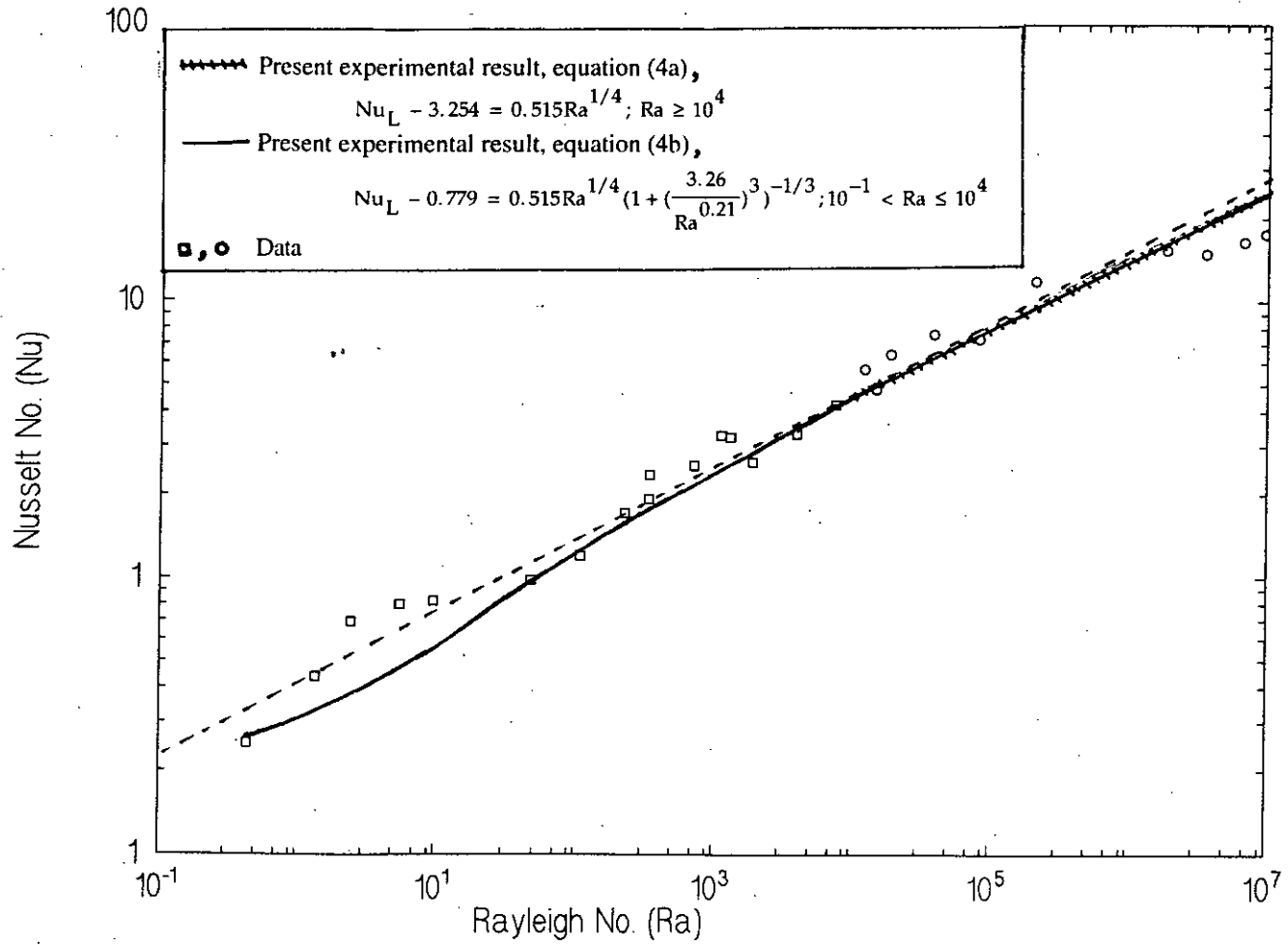


Fig.18 : Plot of Nusselt number Vs. rayleigh number.

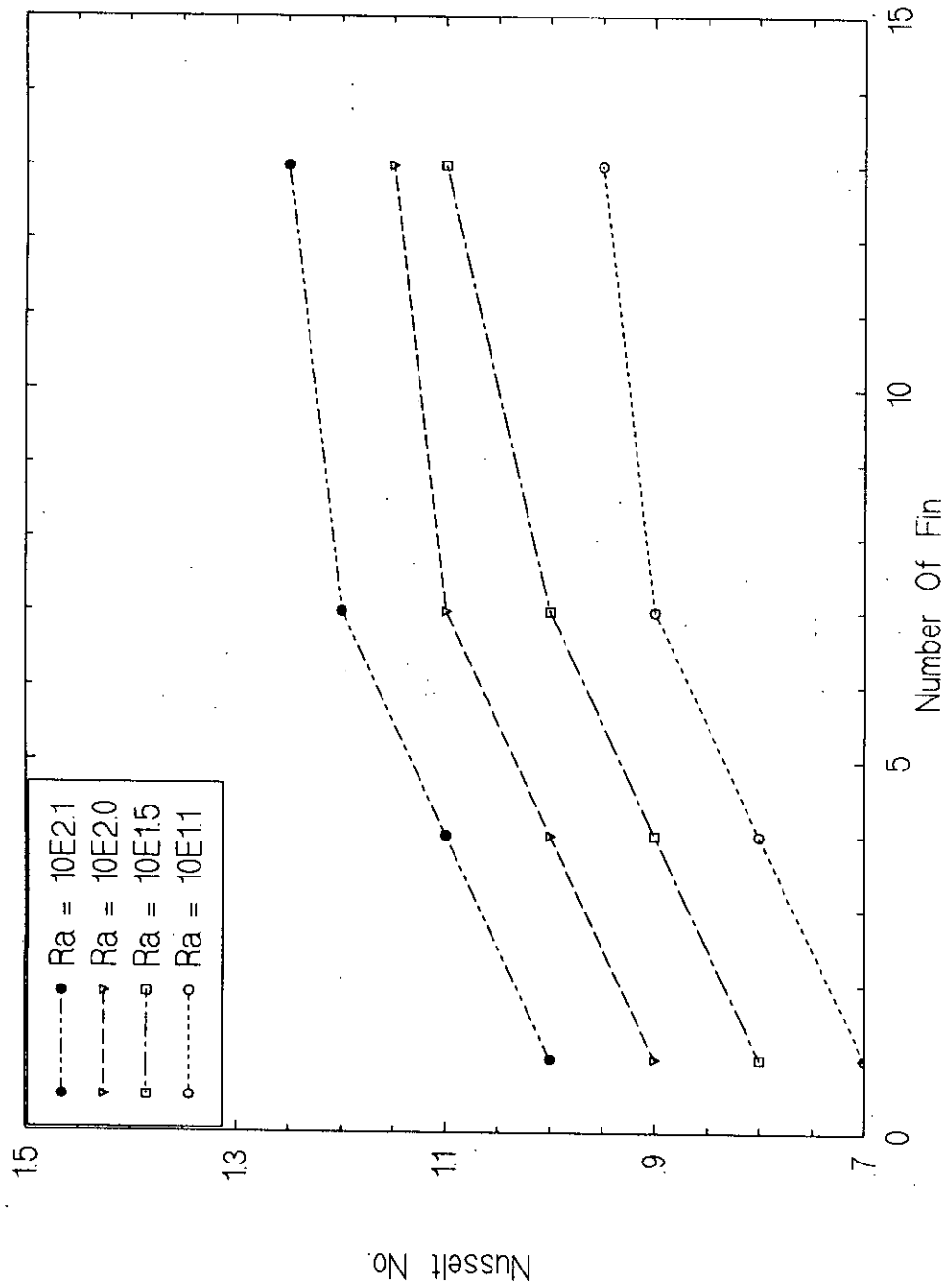


Fig.19 : Effect of fin population on the convective heat transfer.

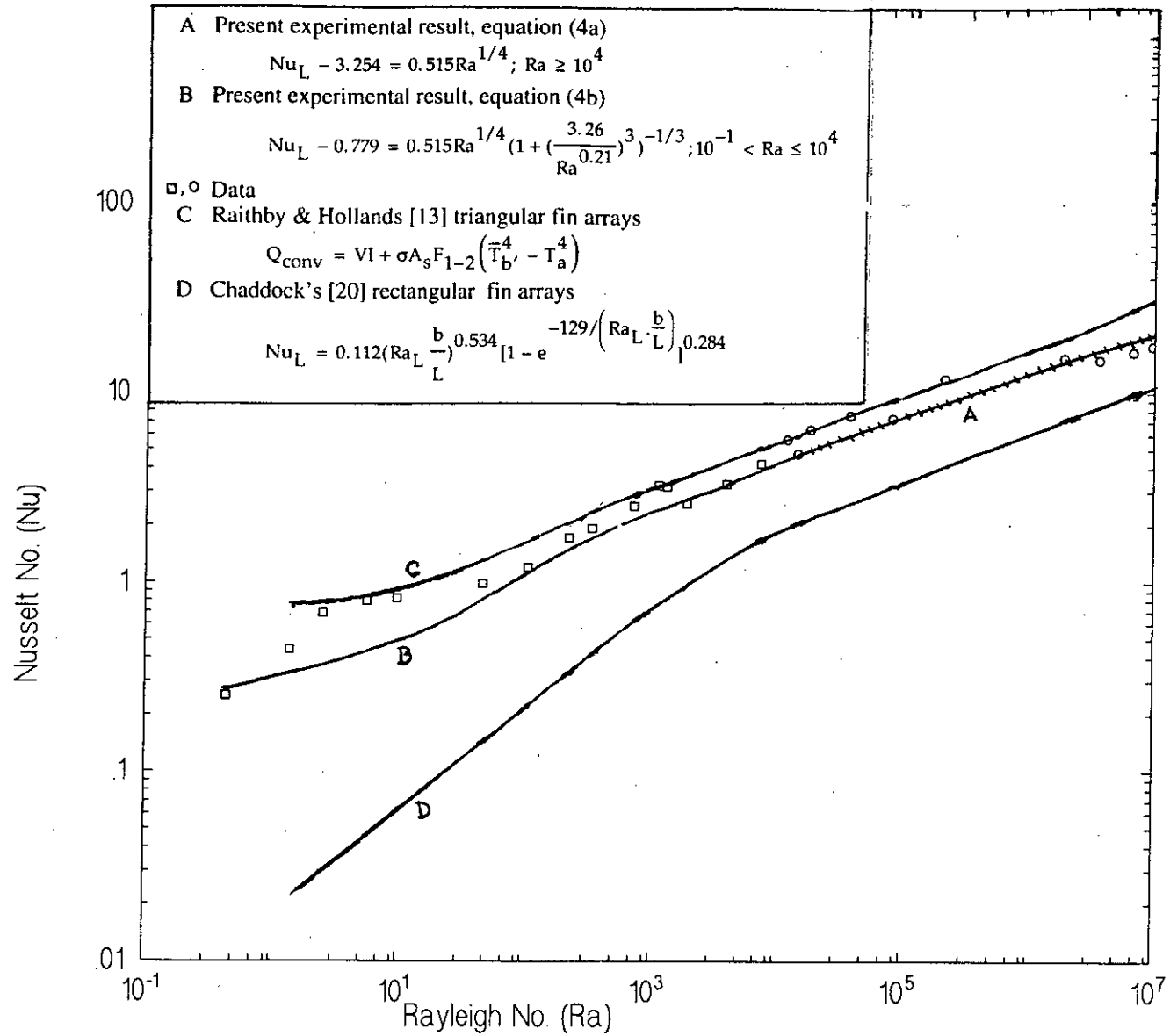


Fig.20 : Comparison of present experimental results with other relevant works

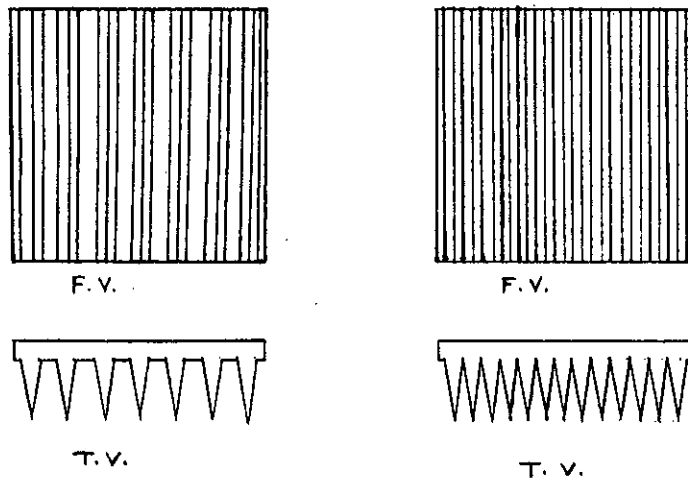
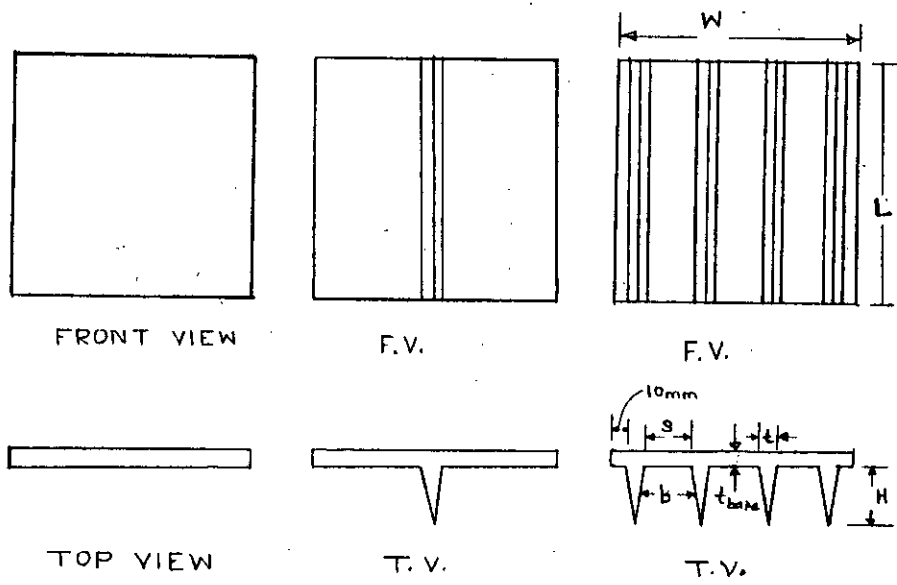
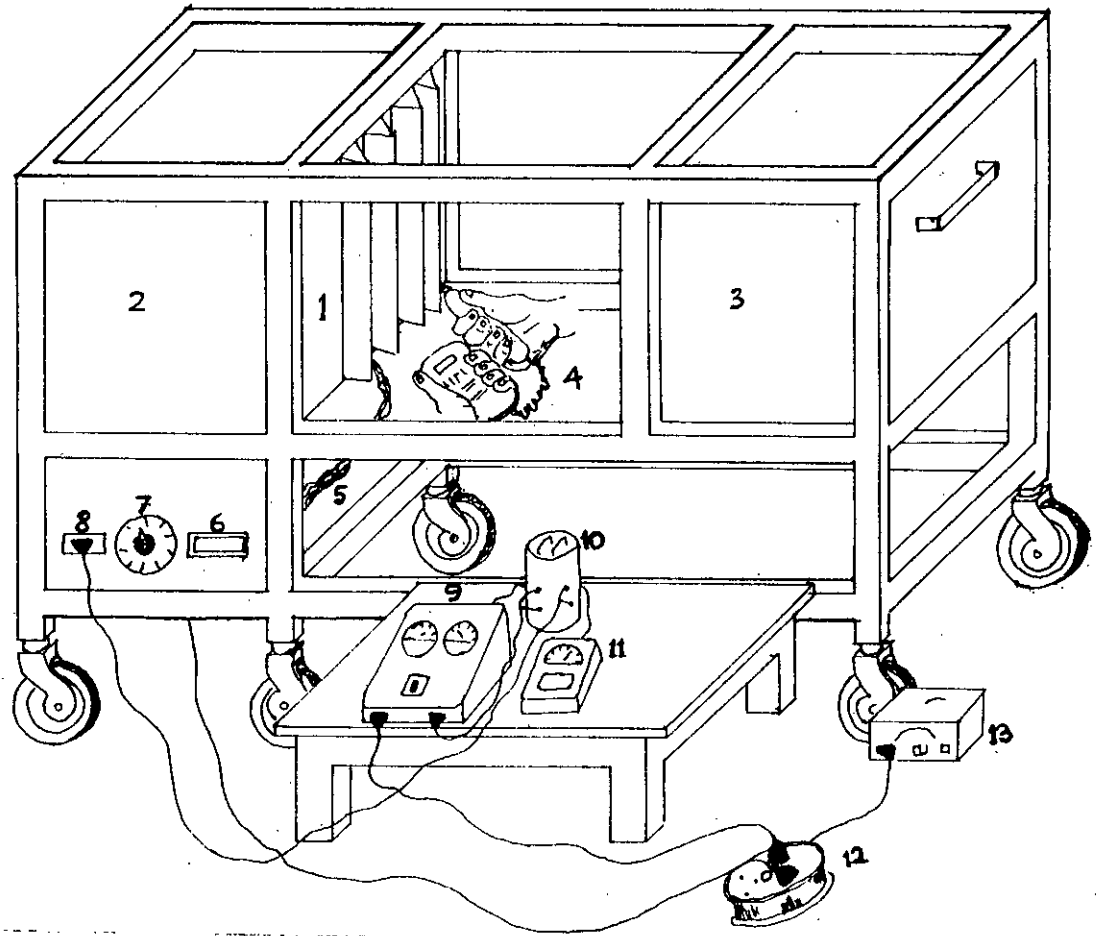


Fig.21: Different Specimen that were used in the Experiment.



- | | | |
|---|--|------------------|
| 1. Specimen | 2. Test Section | 3. Moveable Part |
| 4. Infrared Thermometer | 5. Thermocouple (connected with specimen & selector switch). | |
| 6. Digital Thermometer (connected with selector switch) | | |
| 7. Thermocouple selector switch | 8. Electric Plug for Heater | 9. Voltmeter |
| 10. Voltage regulator | 11. Ammeter | 12. Multi plug |
| 13. Stabilizer | | |

Fig. 22: Schematic Diagram of Experimental Set-up.

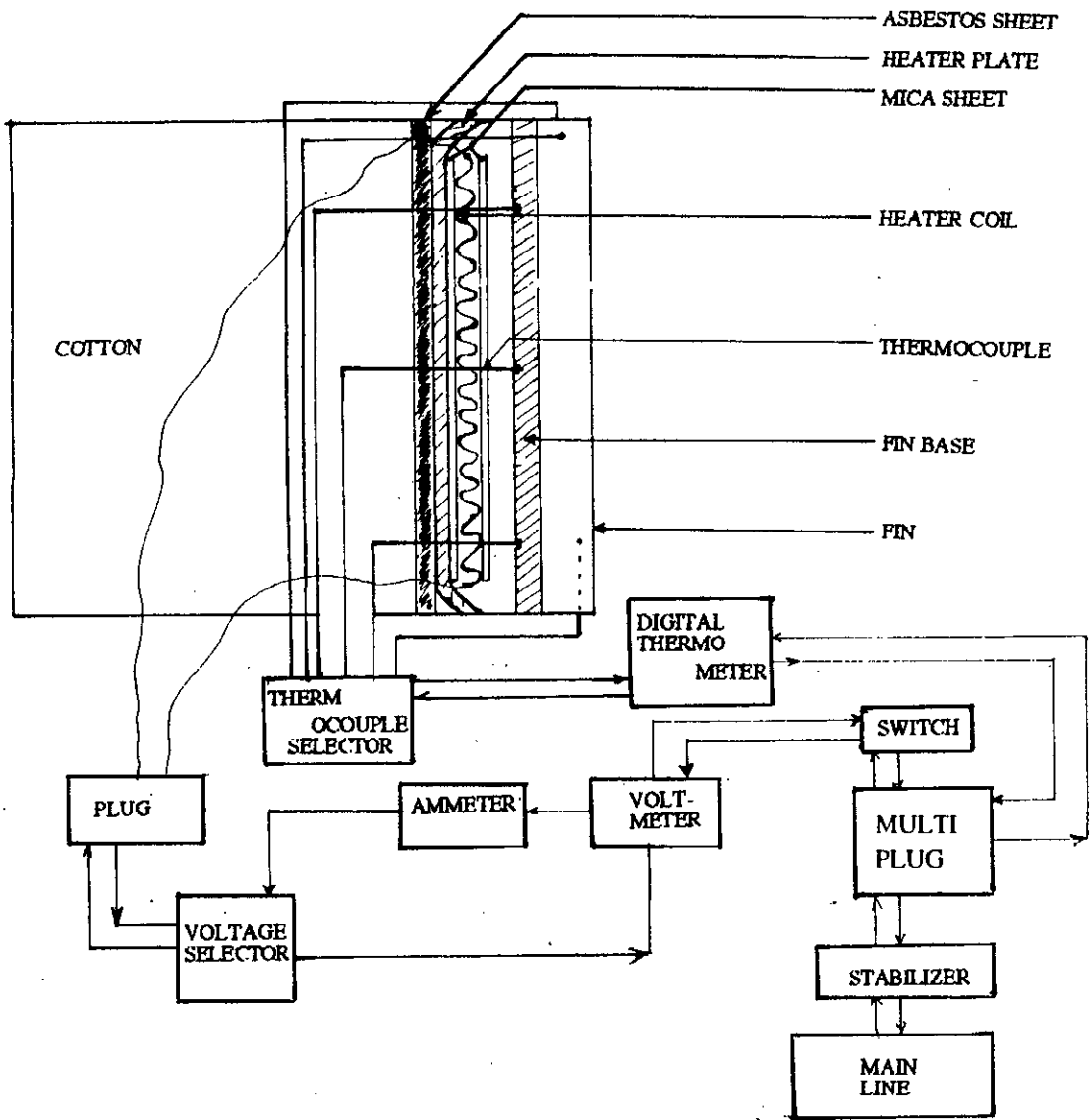


Fig. 23 Details of Test Section.

PARTS NAMES & FUNCTIONS

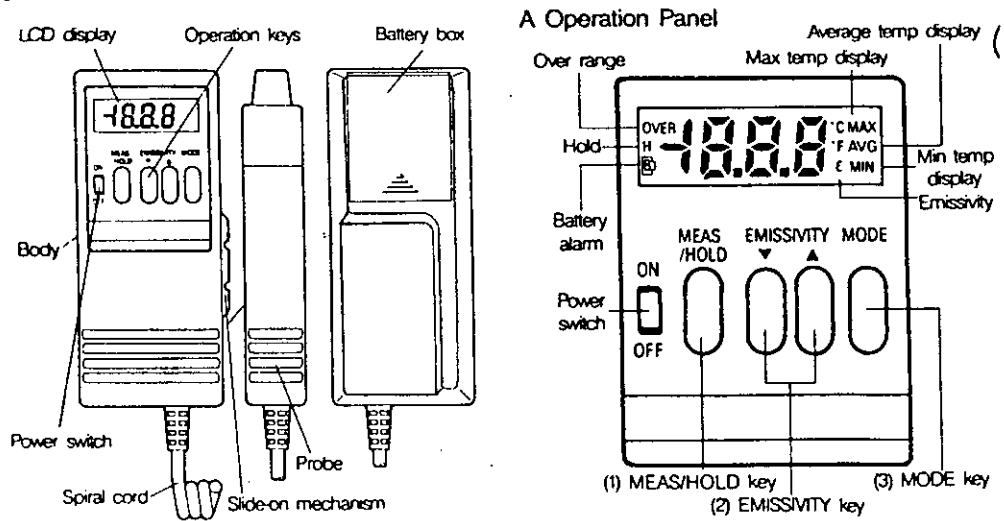


Fig.24: The parts name and functions of the non-contact infrared thermometer.

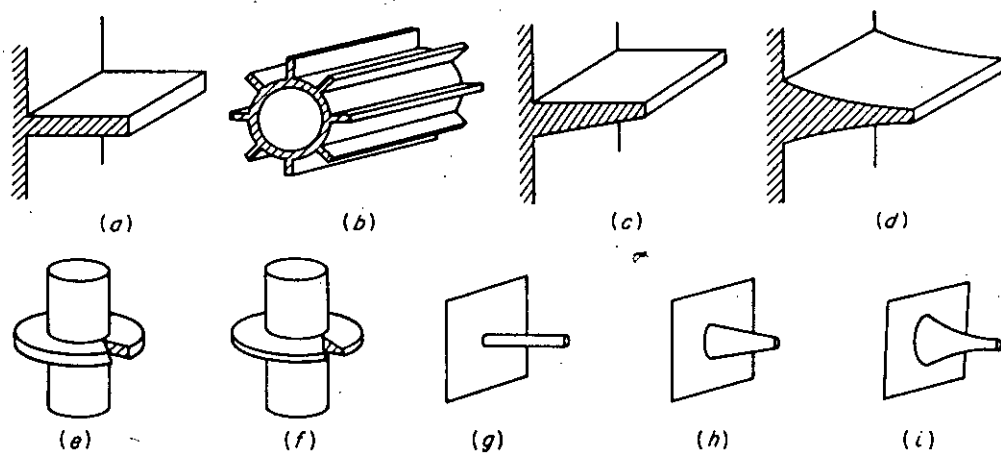


Fig.25: Some typical examples of extended surfaces: (a) Longitudinal fin of rectangular profile; (b) cylindrical tube equipped with fins of rectangular profile; (c) longitudinal fin of trapezoidal profile; (d) longitudinal fin of parabolic profile; (e) cylindrical tube equipped with radial fin of rectangular profile; (f) cylindrical tube equipped with radial fin of truncated conical profile; (g) cylindrical spine; (h) truncated conical spine; (i) parabolic spine.

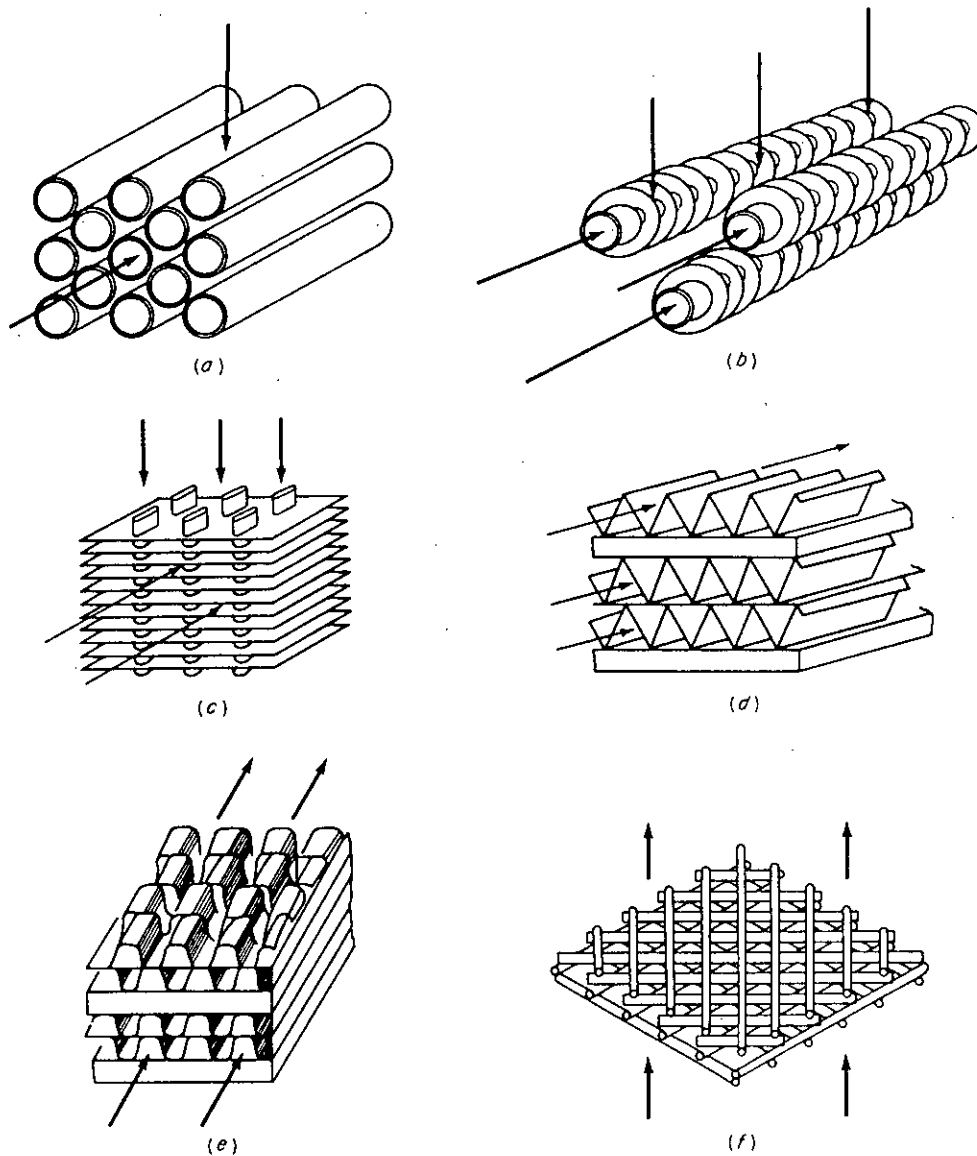


Fig.26: Some typical examples of compact-heat-exchanger surfaces: (a) cylindrical tube; (b) cylindrical tube with cylindrical or radial fins; (c) flat tube with continuous fins; (d) plate fin; (e) offset plate fin; (f) crossed rod matrix.

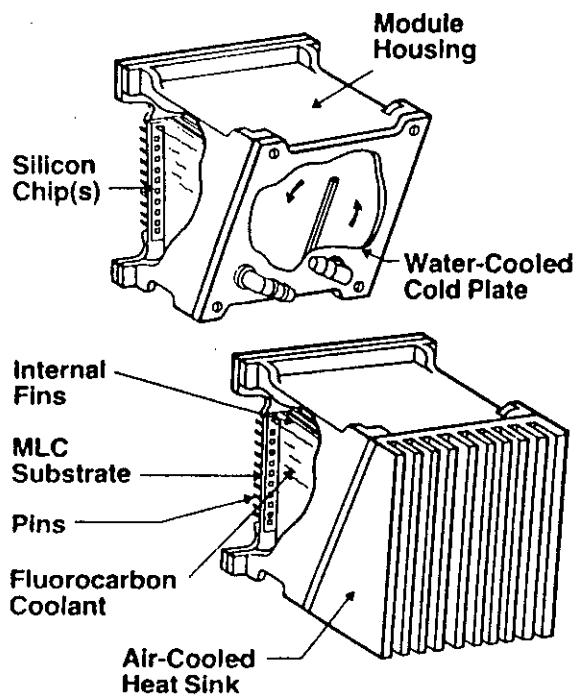


Fig.27a: Natural convection from electronic equipments (IBM's liquid encapsulated modules).

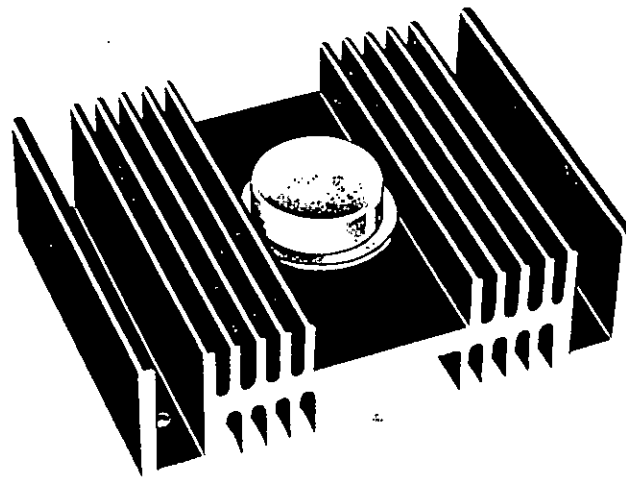
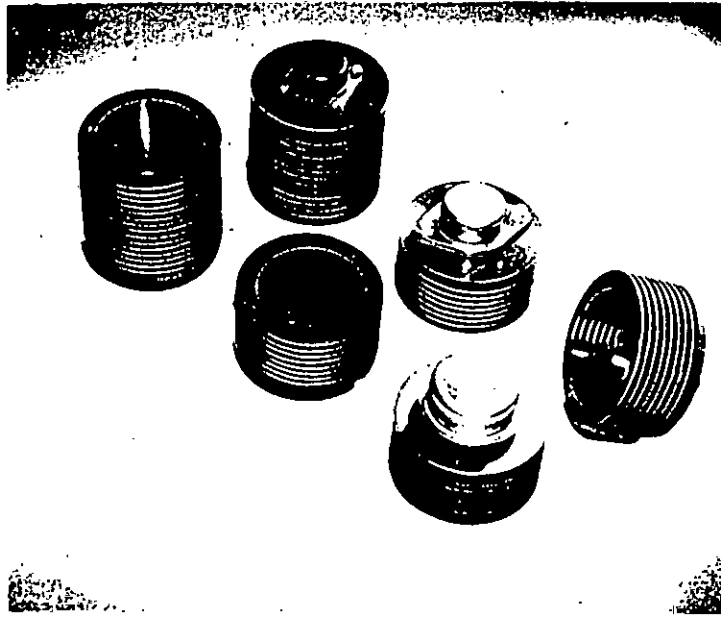


Fig.27b: Transistor heat sinks.

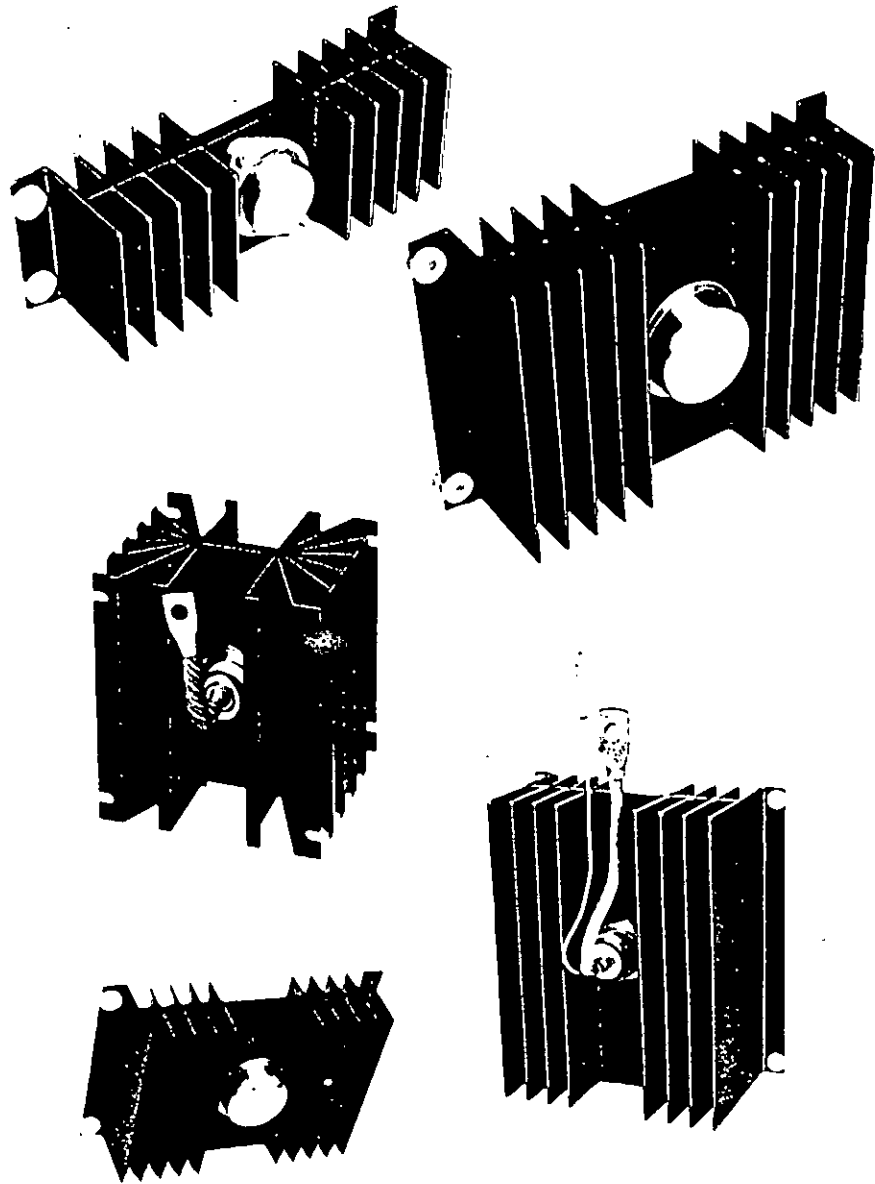


Fig.27c: Transistor coolers.

